ORGANOMETALLICS

Article

pubs.acs.org/Organometallics

Expanding the Family of Hoveyda–Grubbs Catalysts Containing Unsymmetrical NHC Ligands

Veronica Paradiso,[†] Valerio Bertolasi,[‡] Chiara Costabile,[†] Tonino Caruso,[†] Michał Dąbrowski,[§] Karol Grela,[§] and Fabia Grisi*[,†]

[†]Dipartimento di Chimica e Biologia "Adolfo Zambelli", Università di Salerno, Via Giovanni Paolo II 132, I-84084 Fisciano, Salerno, Italy

[‡]Dipartimento di Chimica and Centro di Strutturistica Diffrattometrica, Università di Ferrara, Via L. Borsari 46, I-44100 Ferrara, Italy

[§]Biological and Chemical Research Centre, Faculty of Chemistry, University of Warsaw, Żwirki i Wigury 101, 02-089 Warsaw, Poland

Supporting Information

ABSTRACT: A series of Hoveyda–Grubbs second-generation catalysts containing *N*-alkyl/*N*′-aryl N-heterocyclic carbene (NHC) ligands were synthesized and investigated in representative olefin metathesis reactions. Steric perturbations of unsymmetrical NHCs were achieved through modulation of the hindrance of alkyl (neopentyl, neophyl, cyclohexyl) and aryl (2-isopropylphenyl, mesityl) substituents at the nitrogen atoms in combination with different backbone configurations (*syn* and *anti*). The NHC substitution patterns strongly influence the stability and reactivity of the corresponding complexes. In general, complexes bearing an *anti* NHC backbone are more stable and more active than their corresponding *syn* isomers. In both the series, the presence of bulky, highly branched *N*-alkyl groups tends to give reduced catalytic differences between *syn* and *anti* isomers, whereas the nature of the *N*′-aryl substituent (2-isopropylphenyl or mesityl) gives rise to different activity and/or selectivity. Of note, an *N*′-mesityl catalyst with *anti* backbone was found to be highly competent in the ethenolysis of ethyl oleate, achieving up to 90% selectivity for the formation of terminal olefins.

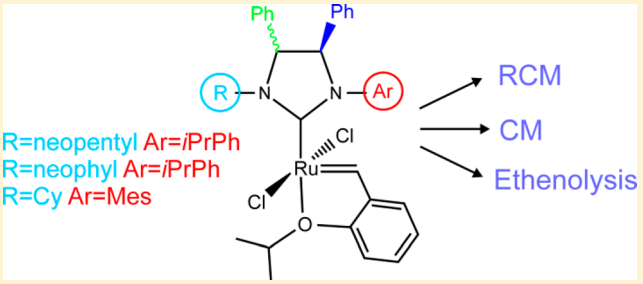

INTRODUCTION

The past few years have seen significant advances in the chemistry of olefin metathesis,[1] mostly due to the development of easily handled, highly efficient NHC-based ruthenium catalytic systems (second-generation catalysts),[2] which have found successful applications in the synthesis of natural products and pharmaceuticals as well as in the production of fine chemicals and oleochemicals.[1,3] The catalytic behavior of this class of ruthenium complexes can be easily modulated through judicious modification of the stereoelectronic properties of the NHC ligand.[4] For example, the introduction of substituents on the backbone of symmetrical NHCs with reduced bulk on the nitrogen atoms has led to the development of ruthenium complexes with enhanced stability toward decomposition pathways via C–H activation of *N*-aryl substituents and high efficiency in the formation of hindered olefins.[5] On the other hand, the advent of unsymmetrical NHC (uNHC) frameworks, whose fascination lies mainly in the possibility that they offer to strongly differentiate the steric bulkiness around the metal, have permitted an increase in catalyst activity and selectivity in several metathesis processes.[6] In this view, the catalytic potential of ruthenium complexes coordinated with uNHCs, especially those presenting one aliphatic and one aromatic amino side group,[7] has been investigated by many researchers (e.g., **1**–**6**, Chart 1). Successful results in specific metathesis applications, such as

Chart 1. Selected Examples of Ruthenium Catalysts with Unsymmetrical NHCs

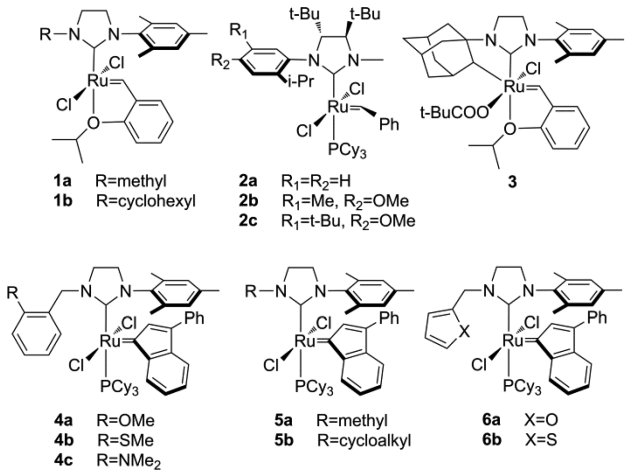

Received: June 27, 2017

DOI: 10.1021/acs.organomet.7b00488
Organometallics XXXX, XXX, XXX–XXX

asymmetric reactions,[6d,8] synthesis of alternating copolymers,[9] selective formation of cyclic oligomers,[10] ethenolysis reactions,[7d,9b] *Z*-selective metathesis transformations,[6c,d,11] and diastereoselective ring rearrangement metathesis,[7e,12] have been achieved.

We have recently proposed an additional strategy for tuning the catalytic properties of this class of complexes, based on the introduction of substituents on the backbone of unsymmetrical NHC moieties in a precise stereochemical arrangement (*syn* or *anti*) (**7**–**10**, Chart 2). Through this structural modification, as

Chart 2. Ruthenium Catalysts with Backbone-Substituted uNHCs

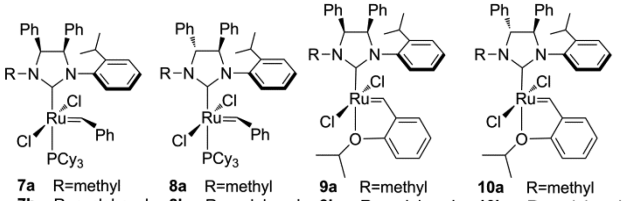

previously observed for analogous systems bearing symmetrical NHCs,[5c–e] ruthenium complexes showing different catalytic behaviors depending on the NHC backbone configuration (*anti* or *syn*) and on the bulkiness of the *N*-alkyl substituent (*N*-cyclohexyl vs *N*-methyl) were obtained.[13]

To further investigate the effect on catalyst properties of unsymmetrical NHCs that combine stereogenic centers on the backbone with differently encumbered *N*-alkyl/*N*′-aryl substituents, we focused our attention on the development of new Hoveyda–Grubbs type complexes (**11a**–**c** and **12a**–**c**, Chart 3) with modified *N*-substituents. In particular, *syn* and *anti*

Chart 3. New Ruthenium Catalysts Bearing uNHCs with Different Backbone Configurations[a]

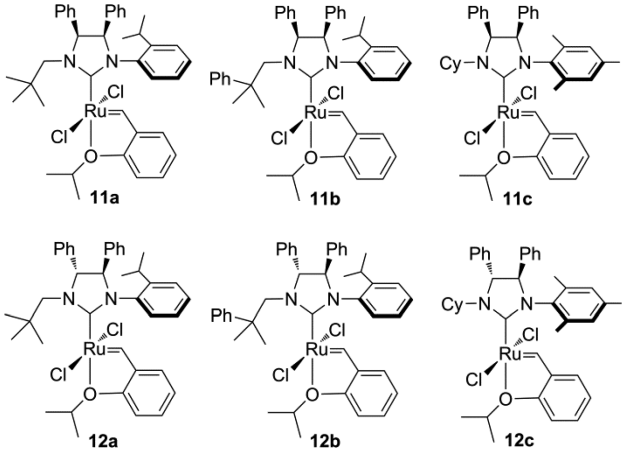

[a]Catalysts **11a**–**c** are racemic mixtures (only one of the enantiomers is depicted), while **12a**–**c** are enantiopure.

NHC backbone substituted complexes possessing an *N*-neopentyl or *N*-neophyl moiety mixed with an *N*′-2-isopropylphenyl group (**11a**,**b** and **12a**,**b**), as well as the analogues having *N*-cyclohexyl/*N*′-mesityl substituents (**11c** and **12c**), were prepared and structurally characterized. The catalytic performances of **11a**–**c** and **12a**–**c** were evaluated in standard metathesis reactions and compared with those of previously reported catalysts **9b** and **10b**, presenting the most significant reactivity difference between *syn* and *anti* isomers. Furthermore, the catalytic potential of all these complexes was explored in a specific metathesis application such as ethenolysis of fatty acid esters, whereas the enantioselective ability of chiral catalysts **12a**–**c** was investigated in model asymmetric ring-closing metathesis (ARCM) and asymmetric ring-opening cross-metathesis (AROCM) reactions.

RESULTS AND DISCUSSION

Synthesis and Characterization of Complexes 11a–c and 12a–c. The new complexes **11a**–**c** and **12a**–**c** were easily obtained by following the synthetic procedures illustrated in Schemes 1 and 2, respectively.[13a] Diamines **13**, **14**, and **17** were

Scheme 1. Synthesis of Ruthenium Complexes 11a–c[a]

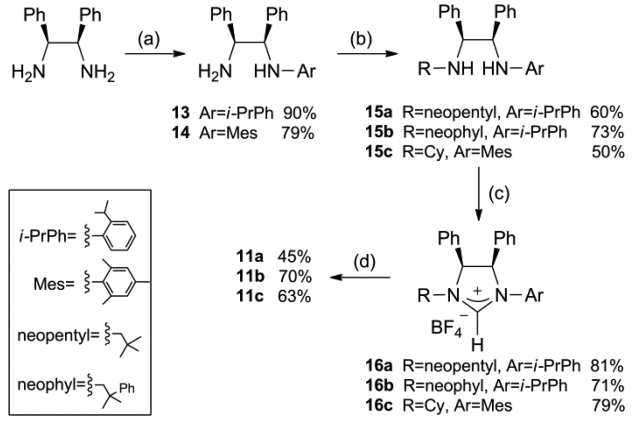

[a]Reaction conditions: (a) *meso*-1,2-diphenylethylenediamine, 2-isopropylbromobenzene (for **13**) or 2-bromomesitylene (for **14**), $Pd(OAc)_2$, NaOtBu, BINAP, toluene, 100 °C, 12 h; (b) (1) $R(CH_3)_2CCHO$ (R = Me, Ph) or cyclohexanone, CH_2Cl_2, molecular sieves, room temperature, 48 h (for **15a**) or 5 days (for **15b** and **15c**), (2) $NaBH_4$, CH_3OH, room temperature, 3.5 h; (c) NH_4BF_4, $CH(OEt)_3$, 135 °C, 2 h (for **15a** and **15c**) or 8 h (for **15b**); (d) $(CF_3)_2CH_3COK$, **HGI**, toluene, 65 °C, 2.5 h.

obtained from the commercial *meso*- or (*R*,*R*)-1,2-diphenylethylenediamine by cross-coupling with 2-isopropylbromobenzene or 2-bromomesitylene and subsequent reductive amination of the appropriate aldehyde or ketone (50–79% yields), whereas diamine **18** was prepared by installing first the cyclohexyl and then the mesityl group (51% yield) on the nitrogen atoms of the starting (*R*,*R*)-1,2-diphenylethylenediamine. After cyclization of the diamines so obtained in the presence of triethyl orthoformate and ammonium tetrafluoroborate, the resulting NHC salts (71–90% yields) were deprotonated in situ with $(CF_3)_2(CH_3)COK$ and reacted with $RuCl_2(=CH\text{-}o\text{-}i\text{PrO-Ph})(PCy_3)$ (**HGI**) to afford the desired complexes **11a**–**c** and **12a**–**c** as air- and moisture-stable solids, in yields ranging from moderate to good (45–70%). It should be underlined that complexes **11a**–**c** are racemic mixtures, while **12a**–**c** are enantiopure.

All of the final products were characterized by 1D and 2D NMR techniques and ESI-FT-ICR analysis.

Crystals suitable for X-ray diffraction analysis were obtained for complexes **11a**,**c** and **12c**, and their crystal structures are shown in Figure 1. A selection of bond distances and angles is given in the Table S2 in the Supporting Information.

DOI: 10.1021/acs.organomet.7b00488
Organometallics XXXX, XXX, XXX–XXX

Scheme 2. Synthesis of Ruthenium Complexes 12a−c[a]

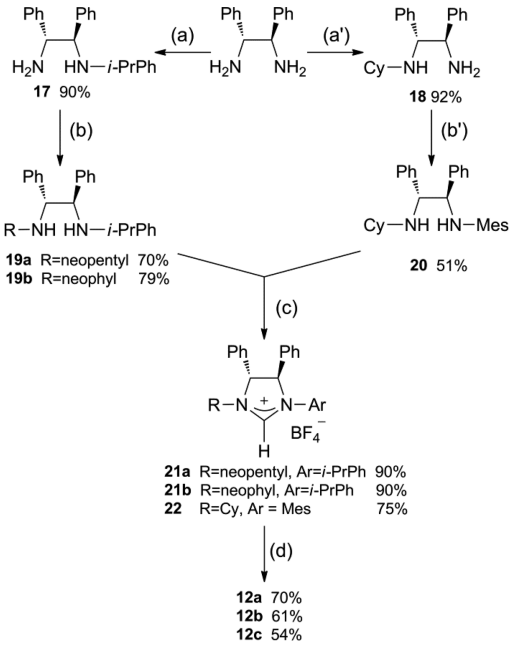

[a]Reaction conditions: (a) (*R*,*R*)-1,2-diphenylethylenediamine, 2-isopropylbromobenzene $Pd(OAc)_2$, NaOtBu, BINAP, toluene, 100 °C, 12 h; (a′) (1) (*R*,*R*)-1,2-diphenylethylenediamine, cyclohexanone, CH_2Cl_2, molecular sieves, room temperature, 14 h, (2) $NaBH_4$, CH_3OH, room temperature, 3.5 h; (b) (1) $R(CH_3)_2CCHO$ (R = Me, Ph), CH_2Cl_2, molecular sieves, room temperature, 14 h (for **19a**) or 5 days (for **19b**), (2) $NaBH_4$, CH_3OH, room temperature, 3.5 h; (b′) 2-bromomesitylene, $Pd(OAc)_2$, NaOtBu, BINAP, toluene, 100 °C, 48 h; (c) NH_4BF_4, $CH(OEt)_3$, 135 °C, 2 h (for **19a** and **20**) or 8 h (for **19b**); (d) $(CF_3)_2CH_3COK$, **HGI**, toluene, 65 °C, 2.5 h.

In all compounds the Ru center is pentacoordinated and adopts a distorted-square-pyramidal coordination geometry. The Cl atoms are trans-oriented in the basal plane and the carbene C1 atom is in a trans position with respect to the O1 oxygen of the 2-*i*PrO substituent at the benzylidene ligand, which is almost coplanar with the NHC ring, being rotated by only 8.80(8), 11.20(13), and 3.13(8)° for the three complexes **11a,c** and **12c**, respectively.

Compound **11a** crystallizes in the centrosymmetric $P2_1/n$ space group with the NHC phenyl groups in *cis* positions with respect to the C2−C3 bond. Accordingly, the crystal contains a racemic mixture of both the enantiomers having opposite configurations (*SR* or *RS*) at the C2 and C3 asymmetric carbon atoms. The conformations of the substituents at the N1 and N2 NHC atoms are mainly determined by short intramolecular interactions: H14b···Ru1 = 2.54 Å and H4···(centroid of C19/C24 phenyl ring) = 2.40 Å.

Complexes **11c** and **12c** are isomers with different relative configurations at the C2 and C3 atoms of NHC group. Both crystallize in the noncentrosymmetric *C*2 space group. In **11c** the phenyl groups, bonded to C2 and C3 of the NHC ring, are in *cis* positions. Accordingly, the C2 and C3 carbons display opposite configurations: *S* and *R*, respectively. Conversely, in complex **12c** the phenyl groups at C2 and C3 are in trans positions and the C2 and C3 carbon atoms of NHC display the same *R* chirality. The absolute configurations could be determined reliably from the crystallographic data, using the calculated Flack parameters[14] of 0.00(2) and −0.03(2) for complexes **11c** and **12c**, respectively.

The conformations of the substituents at the N1 and N2 of the NHC rings are controlled by short intramolecular interactions between the C4−H4 group of the benzylidene moiety and the centroid of the C20/C25 phenyl ring, as well as by interactions between the C14−H14 group of the cyclohexyl substituent and the Ru atom. The C−H···π interactions between the C4−H4 group and the centroids ***C*** of the C20/C25 phenyl rings are characterized by the following parameters H4···***C***(C20/C25) = 2.70 and 2.58 Å and C4−H4···***C*** = 162 and 168°, for **11c** and **12c**, respectively. Furthermore, the short C−H···Ru interactions display H14···Ru1 distances of 2.51 and 2.50 Å and C14−H14···Ru1 angles of 122 and 123° for complexes **11c** and **12c**, respectively.

Before investigating the catalytic behavior of the newly developed complexes, their thermal stability was studied. C_6D_6 solutions (0.01 M) of each complex, prepared under a nitrogen atmosphere and containing tetrakis(trimethylsilyl)silane as an internal standard, were heated at 60 °C for 1 month and monitored by ^{1}H NMR spectroscopy. Stability tests performed during the first 14 days are illustrated in Figure 2. After 1 week, *syn* complexes **11a,b** were found to be almost completely decomposed (only 4% of initial complexes remained), while their corresponding *anti* isomers **12a,b** exhibited a greater stability, as they decomposed within 12 and 10 days, respectively. Moreover, decomposition rates are very similar for **11a,b** but are significantly different for **12a,b**, suggesting a major effect of the *N*-alkyl substitution on complex stability in the presence of an *anti* NHC backbone configuration. This is observed also for reference complexes **9b** and **10b**, where the presence of the *N*-cyclohexyl group ensures major stability with respect to catalysts **11a,b** and **12a,b**, allowing detection, after 14 days, of 32% of **9b** and 42% of **10b** unaltered. At 1 month, 26% of *anti* isomer **10b** still persisted, while only 8% of *syn* **9b** remained. On the other side, the presence of a more bulky *N*′-aryl substituent such as a mesityl group resulted in outstanding stability of the resulting complexes **11c** and **12c**, which indeed both showed no decomposition within 1 month, also proving to be more robust than the classical, commercially available **HGII** catalyst[16] bearing a symmetrically aryl substituted NHC.[17]

As reported in the literature, the stability of unsymmetrical catalysts is associated with the nature of NHC *N*-substituents.[7f,18] In a recent study on NHC-Al complexes the stability was attributed to steric factors,[19] by using topographic maps and $\%V_{Bur}$ as steric parameters.[20] $\%V_{Bur}$ is a well-known parameter, successfully used to quantify the steric hindrance of NHC ligands by measuring the amount of volume of a sphere centered on the metal, buried by overlap with atoms of the ligand.[21] Bulkier ligands occupy a larger amount of that sphere and present greater $\%V_{Bur}$ values.

To observe if the decomposition of our complexes could be correlated to the steric NHC encumbrance, topographic maps (Figure 3) and $\%V_{Bur}$ of complexes **9b**, **10b**, **11a−c**, and **12a−c** were calculated. Since no X-ray were available for complexes **11b** and **12a,b**, we used DFT minimum energy optimized structures for all complexes for topographic maps and $\%V_{Bur}$ calculations. $\%V_{Bur}$ could be sensitive to the conformations of the *N*-alkyl group; nevertheless the only complexes that could present reasonable additional low-energy structures are **11b** and **12b** bearing *N*-neophyl substituents, due to the rotation around the C−C single bond that changes the position of the Ph group. The only significant degree of freedom for *N*-cyclohexyl and *N*-neopentyl groups lies in rotation around N−C bond, but in both cases it is difficult to imagine different low-energy

DOI: 10.1021/acs.organomet.7b00488
Organometallics XXXX, XXX, XXX−XXX

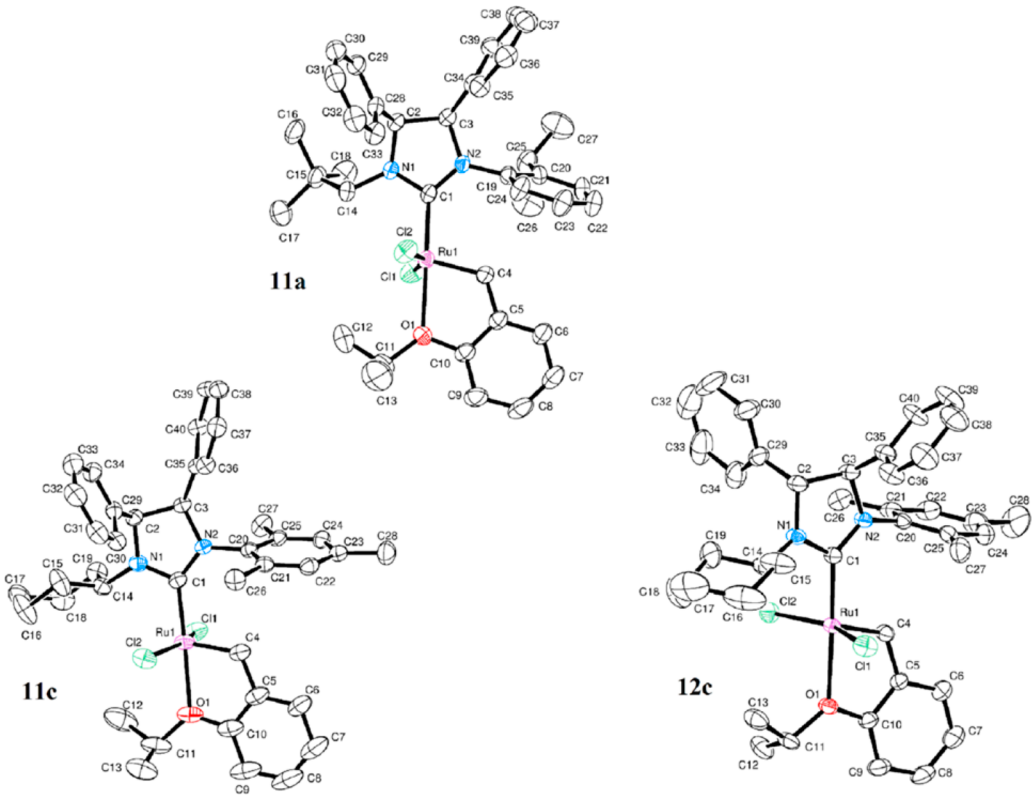

Figure 1. ORTEP[15] views of compounds **11a,c** and **12c** showing the thermal ellipsoids at the 40% probability level.

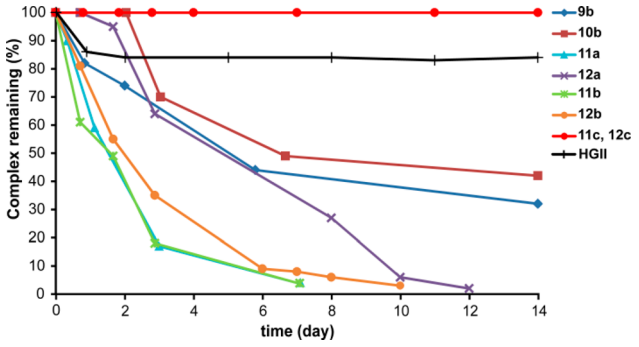

Figure 2. Thermal stability in C_6D_6 at 60 °C under nitrogen of Ru complexes **11a−c** and **12a−c**. Decomposition was monitored by ^{1}H NMR spectroscopy using tetrakis(trimethylsilyl)silane as an internal standard. The lines are intended as a visual aid only.

structures. For the *N*-neopentyl group, which could adopt apparently more conformations, the orientation is imposed by the phenyl groups on the backbone. Minimum energy structures of **11b** and **12b** involve a partial π-stacking interaction between the phenyl substituent on the backbone and the phenyl of the neophyl group (Figure 4). Different conformations without π stacking were explored for the last two complexes. Nevertheless, the best optimized structures present internal energies increases of 1.6 and 1.8 kcal/mol for **11b** and **12b**, respectively, and did not show dramatic differences in topographic maps and $\%V_{Bur}$, the phenyl group of neophyl being far from the metal center. Topographic maps and structures of these conformations are reported in the Supporting Information.

In Table 1, the percentages of undecomposed complex after 3 days, the values of $\%V_{Bur}$ representative of the most hindered quadrant ($\%V_{Bur}$ Max), and the overall $\%V_{Bur}$ values are reported.

According to topographic maps, higher steric hindrance is concentrated on the *N*-alkyl substituent side, which is always located far from the alkylidene. **11c** and **12c**, presenting the highest $\%V_{Bur}$, were also shown to be the most stable complexes. Nevertheless, according to the data in Table 1 the complex stability seems more correlated to the $\%V_{Bur}$ Max value (representative of the most hindered quadrant). The lower the $\%V_{Bur}$ Max, the lower the stability shown by the complex. In order to give a more comprehensive overview, data for complex **HGII** from DFT optimization (see the Supporting Information) are also reported in Table 1 even if we did not expect a behavior in line with that of the examined catalysts due to the different nature of NHC ring substitution. Concerning the nature of the deactivating species and the mechanisms of deactivation, it is hard to reach a conclusion. Indeed, although for symmetrical NHCs bearing *N*-aryl substituents with low hindrance decomposition via C−H activation is well documented,[22] for complexes **9b**, **10b**, and **11a−c**, presenting a mono-ortho-substituted *N*-aryl group, a careful check of the distances between the *o*-CH bond and Ru suggests no correlation between these distances and the stability of the complexes. On the other hand, it is worth noting that decomposition pathways of olefin metathesis catalysts bearing NHC ligands with *N*-alkyl groups are still quite unknown. To the best of our knowledge, the only examples are related to cyclometalated ruthenium benzylidene complexes reported by Grubbs (e.g., **3**, Chart 1), formed through a carboxylate-assisted C−H activation.[23]

The electrochemical behavior of **9b**, **10b**, **11a−c**, and **12a−c** was also investigated to gain useful information about the electron-donating properties of the NHC ligand coordinated to

DOI: 10.1021/acs.organomet.7b00488
Organometallics XXXX, XXX, XXX−XXX

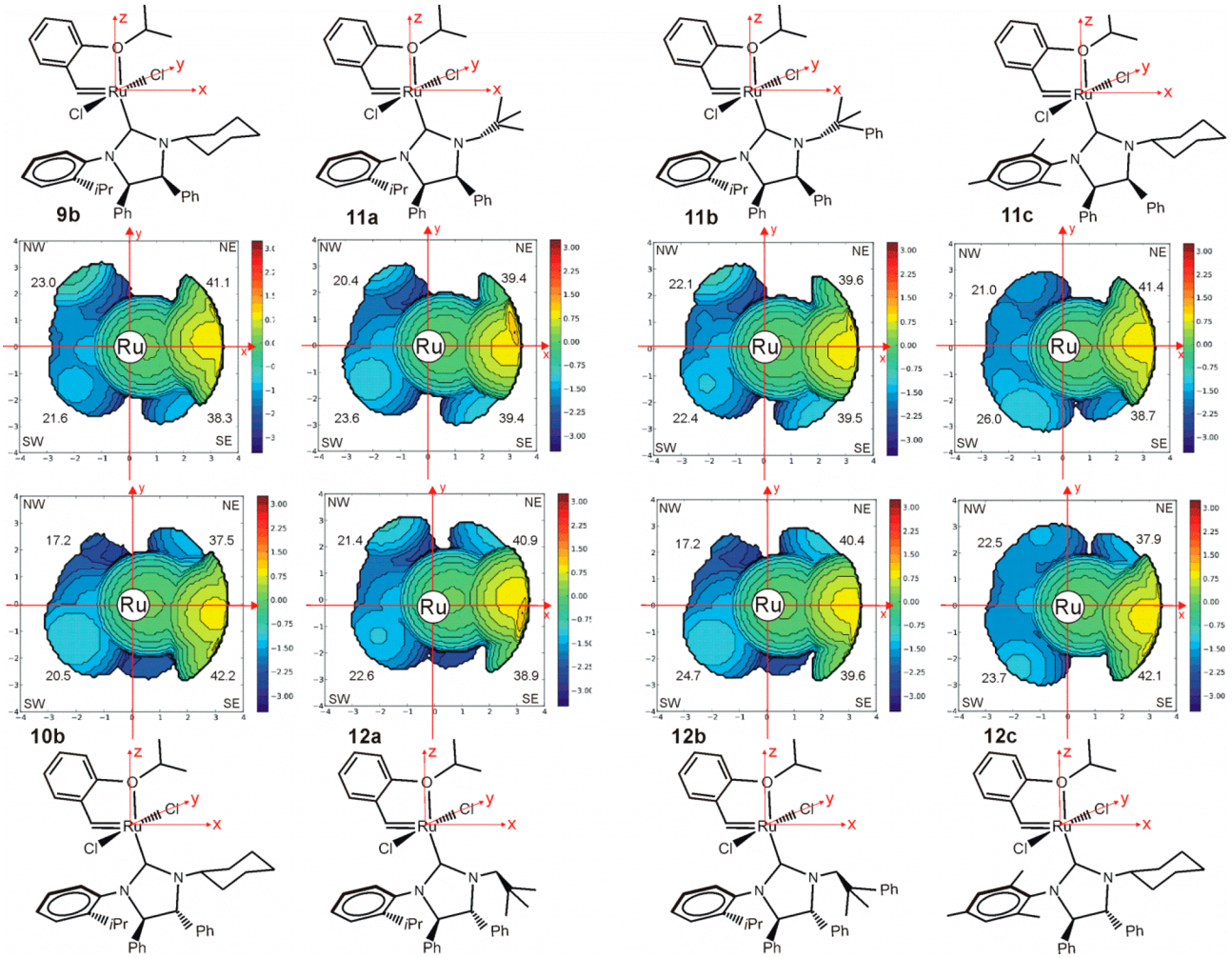

Figure 3. Topographic steric maps of **9b**, **10b**, **11a−c**, and **12a−c**. The iso-contour curves of steric maps are given in Å. The maps were achieved by starting from minimum energy structures of complexes optimized by DFT calculations. The complexes are oriented according to the complex scheme of the corresponding map. $\%V_{Bur}$ representative of each single quadrant is reported for each map.

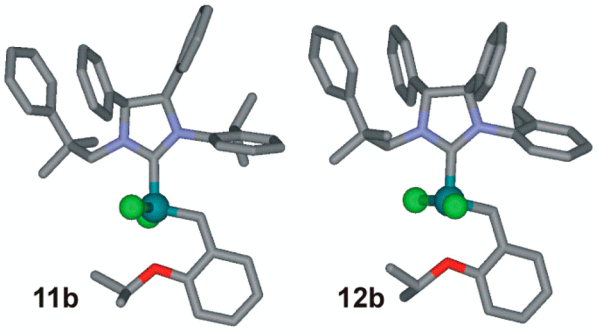

Figure 4. DFT optimized structures of complexes **11b** and **12b**.

the metal.[24] The Ru(II)/Ru(III) redox potentials derived by cyclic voltammetry are reported in Table 2.

The values registered for complexes **9b**, **10b**, **11c**, and **12c** bearing an *N*-cyclohexyl group are quite similar, varying in a range of only 3−13 mV, and no clear trend depending on the NHC backbone configuration and/or the nature of the *N*′-aryl substituent was observed. For complexes **11a**,**b** and **12a**,**c** with a branched *N*-alkyl substituent, differences in redox potentials are even less significant (3−8 mV), indicating a negligible role not only of the *N*-substitution but also of the relative orientation of substituents on the backbone. On the whole, electronic properties of uNHCs coordinated to the examined complexes seem to be influenced very little by the types of substitution patterns. The lowest redox potential values, reflecting the highest electron density at the metal center, are observed for complexes **9b** and **12c**, characterized by an *N*-

Table 1. Percentage of Undecomposed Complex after 3 Days, value of the $\%V_{Bur}$ Representative of the Most Hindered Quadrant ($\%V_{Bur}$ Max), and Value of the Overall $\%V_{Bur}$ and for 9b, 10b, 11a−c, and 12a−c

complex	complex (%)[a]	$\%V_{Bur}$ Max[b]	$\%V_{Bur}$
11a	17	39.4	30.7
11b	18	39.6	30.9
12b	35	40.4	30.5
12a	64	40.9	31.0
9b	68	41.1	31.0
10b	70	42.2	30.5
HGII	84	42.9	32.9
11c	100	41.4	31.8
12c	100	42.1	31.5

[a]Percentage of undecomposed complex after 3 days in C_6D_6 at 60 °C under nitrogen. [b]$\%V_{Bur}$ representative of the most hindered quadrant (NE or SE in Figure 3 depending on the complex shape).

DOI: 10.1021/acs.organomet.7b00488
Organometallics XXXX, XXX, XXX−XXX

Table 2. Redox Potentials of Ruthenium Complexes 9b, 10b, 11a–c, and 12a–c Determined by Cyclic Voltammetry

complex	$\Delta E_{1/2}$ (V)[a]	$E_a - E_c$ (mV)
9b	0.947	73
10b	0.960	102
11a	0.969	102
12a	0.978	112
11b	0.972	98
12b	0.976	112
11c	0.961	98
12c	0.950	83
HGII	0.860[b]	66

[a]Redox potentials determined using cyclic voltammetry in CH_2Cl_2 under nitrogen. Conditions: 1 mM analyte, 0.1 M NBu_4PF_6 as supporting electrolyte, and 1 mM octamethylferrocene as an internal standard. Scan rate: 100 mV/s. [b]Redox potential reported in the literature[20] is 0.850 V.

cyclohexyl group. In comparison to **HGII** catalyst, complexes **9b**, **10b**, **11a–c**, and **12a–c** are anodically shifted by 87–118 mV, underlining a lower donor ability of the corresponding uNHC ligands. This finding was already observed for ruthenium complexes bearing symmetrical NHCs with phenyl groups on the backbone.[25] However, we are not able to unambiguously ascribe the lower donor ability of the examined uNHCs to the backbone substitution or to the nature of the *N*-substituents. Work is in progress to gain more information about this issue.

Ring-Closing Metathesis (RCM) Activity Studies. The catalytic performances of **11a–c** and **12a–c** were first evaluated in RCM reactions of malonate and *N*-tosyl derivatives with different degrees of steric hindrance. All cyclization reactions were carried out at 60 °C in C_6D_6 and monitored by ^{1}H NMR spectroscopy. The corresponding kinetic plots are shown in Figures 5–7, where the conversion–time curves previously determined for the same ring closures promoted by catalysts **9b** and **10b**[13] are also displayed. Comparisons to commercially available **HGII** catalyst are included in the graphs. Further details, are reported in the Tables S3–S5 in the Supporting Information.

In the RCM of diethyl diallylmalonate (**23**, Figure 5A), catalysts **11a,b** and, **12a,b** were able to complete cyclization in a range of 5–8 min, with **12a** emerging as the most efficient system, nearly equaling the best performing catalyst **10b**. However, in contrast to what has been observed for systems containing a flexible cyclohexyl *N*-substituent (**9b**, **10b**), the introduction of bulky, highly branched *N*-alkyl moieties, such as neopentyl or neophyl groups, led to strongly reduced differences between complexes with *syn* and *anti* NHC backbone configuration. Indeed, *anti* complexes **12a,b** showed activities only slightly higher than those of their *syn* congeners **11a,b** (Table S3 in the Supporting Information).

Increasing the steric hindrance of the *N*′-aryl substituent from a 2-isopropyphenyl to a mesityl group (**11c**, **12c**) led to less efficient catalytic systems that, again, exhibited a significant discrepancy between catalytic behaviors of *anti* (98% conversion in 37 min) and *syn* (89% conversion in 60 min) isomers (Table S3 in the Supporting Information). In the RCM of *N*-diallyl tosylamine (**25**, Figure 5B), activities of all the tested catalytic systems were equal or inferior to those observed for the malonate derivative **23**, which typically is more reluctant to undergo cyclization reactions, confirming the tendency of this class of ruthenium catalysts bearing uNHCs to give RCM nonproductive events with less demanding substrates.[13b] In both of the RCM reactions, all of the new catalysts emerged as less active than commercial symmetrical **HGII** used at 10 times lower catalyst loading (Table S3).

The kinetic profiles for the RCM of **27** and **29** promoted by catalysts **11a–c** and **12a–c** are sketched in Figure 6. *Anti* catalysts with neopentyl (**12a**) and neophyl *N*-substituents (**12b**) were able to quantitatively convert **27** in 13 and 10 min, respectively (Figure 6A), proving to be more efficient than their *syn* congeners **11a** and **11b**. In the RCM of the *N*-tosyl derivative **29** (Figure 6B), *N*-neopentyl catalysts **11a** and **12a** showed similar activities (99% conversion within 7 and 5 min, respectively), whereas *N*-neophyl catalysts **11b** and **12b** disclosed a more marked reactivity difference dependent on the NHC backbone configuration. Indeed, *anti* catalyst **12b** quantitatively furnished the cyclic product **30** within 5 min, while *syn* isomer **11b** required 12 min.

In both RCM reactions for the formation of cycloolefins **28** and **30**, the worst performances were given by *N*-cyclohexyl/

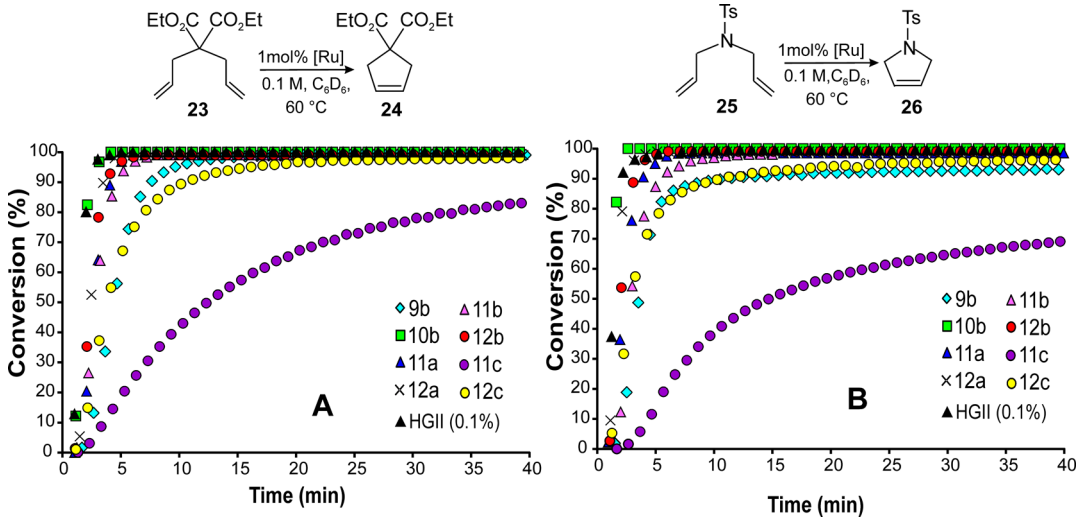

Figure 5. Kinetic profiles for the RCM of **23** (A) and **25** (B).

DOI: 10.1021/acs.organomet.7b00488
Organometallics XXXX, XXX, XXX–XXX

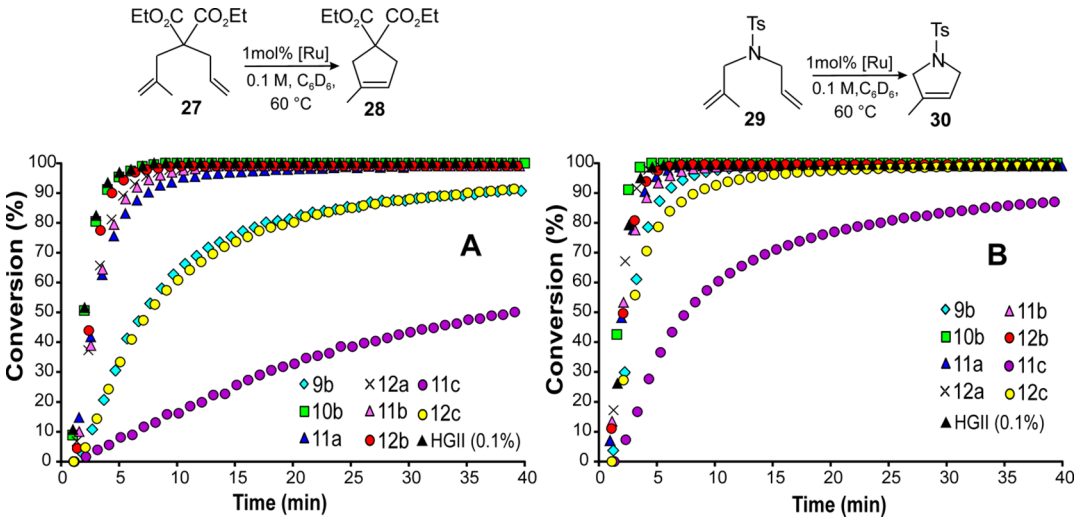

Figure 6. Kinetic profiles for the RCM of **27** (A) and **29** (B).

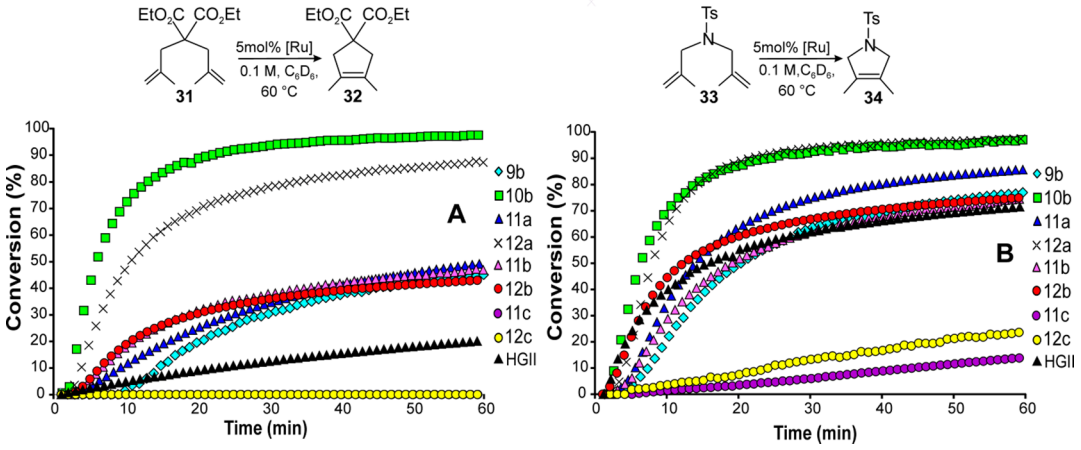

Figure 7. Kinetic profiles for the RCM of **31** (A) and **33** (B).

N′-mesityl catalysts, which, in addition, displayed remarkable differences in the catalytic activity of the *syn* and *anti* isomers. In addition, for these transformations all of the newly synthesized catalysts were revealed to be less efficient than **HGII** (see Table S4 in the Supporting Information).

Finally, we compared the catalytic behaviors of **11a−c** and **12a−c** in the RCM of sterically demanding diolefins **31** and **33** (Figure 7 and Table S5 in the Supporting Information). All of the catalysts were found to perform better in the RCM of *N*-tosyl substrate **33** than in that of malonate substrate **31**. In the RCM of **33**, catalyst **12a** with a neopentyl *N*-group behaved like the best performant **10b** possessing an *N*-cyclohexyl substituent (97% conversion), while it appeared less efficient in the cyclization of **31** (88% vs >97% conversion). The corresponding *syn* isomer **11a** showed lower propensity to effect both cyclizations of **31** and **33**, as also observed for the analoguous *N*-cyclohexyl complex **9b.**

Moving from neopentyl to neophyl as an *N*-substituent was sufficient to render negligible the role of NHC backbone configuration; indeed **11b** and **12b** exhibited comparable catalytic activities. Changing the *N*′-aromatic moiety from 2-isopropylphenyl to mesityl dramatically affected the catalytic behavior, as was clearly shown from an analysis of conversion plots for both RCM reactions carried out with **11c** and **12c**. All of the catalysts having an *N*′-2-isopropylphenyl substituent were found to exhibit better performances in comparison to **HGII** in the RCM of **31** and **33**. However, in the ring closure of **33**, the catalytic activities of **11b** and **12b** presenting a bulky neophyl *N*-substituent were very similar to that of the benchmark commercial catalyst (see Table S5 in the Supporting Information).

For RCM, as well as for other kind of metathesis later discussed in this paper, an important role could be played by the two catalyst sides of unsymmetrical complexes, which would possibly depend on the rate of NHC rotation vs the metathesis reaction. Nevertheless, to the best of our knowledge, there have been no studies clarifying the role of NHC unsymmetrical *N*-substitution. The hypothesis of NHC rotation was explored by Collins in asymmetric metathesis promoted by ruthenium catalysts bearing a chiral C_1-symmetric ligand, but no definitive conclusion was reached. To address this issue, further experimental as well as theoretical studies should be undertaken.[26]

Cross-Metathesis (CM) Activity. The catalytic behavior of newly synthesized catalysts **11a−c** and **12a−c** was then examined in the standard cross-metathesis (CM) reaction of allyl benzene (**35**) and *cis*-1,4-diacetoxy-2-butene (**36**) (Scheme 3). The results are summarized in Table 3 together with the available data for the same reactions performed with catalysts **9b**, **10b**, and **HGII**.

DOI: 10.1021/acs.organomet.7b00488
Organometallics XXXX, XXX, XXX−XXX

Scheme 3. CM of Substrates 35 and 36

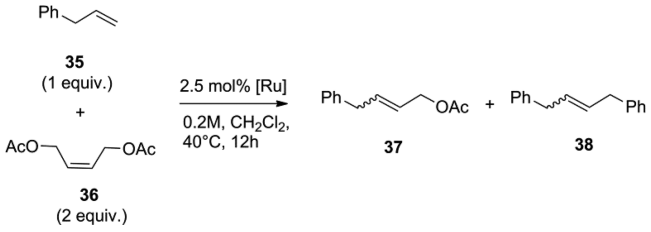

Table 3. CM of 35 and 36 Promoted by Catalysts 11a–c and 12a–c

entry[a]	catalyst	isolated yield of **37** (%)	*E*/*Z*[b]	isolated yield of **38** (%)	*E*/*Z*[b]
1	**9b**	72	2.6	23	5.5
2	**10b**	67	7.6	28	5.7
3	**11a**	78	3.0	19	5.0
4	**12a**	80	7.6	11	6.1
5	**11b**	80	4.2	20	4.5
6	**12b**	69	7.7	7	6.6
7	**11c**	50	3.9	38	5.2
8	**12c**	89	4.4	11	5.8
9	**HGII**	69	8.6	15	5.3

[a]Reactions in CH_2Cl_2 at 40 °C for 12 h, catalyst 2.5 mol %. [b]*E*/*Z* ratios were determined by ^{1}H NMR spectroscopy.

All catalysts were found to be competent in the examined CM reaction, giving only cross-metathesis (**37**) and homometathesis (**38**) products. No byproducts arising from double-bond isomerization were observed. Replacement of a cyclohexyl group by a neopentyl or neophyl group as *N*-substituent proved to have little effect on the activity and selectivity of the corresponding catalysts (Table 3, entries 1–6), confirming a major tendency of complexes with a *syn* backbone configuration to give lower *E*/*Z* ratios in comparison to their *anti* analogues[13] that indeed behave like commercial **HGII** (entry 9). On the other hand, *anti* complexes **12a**,**b** with highly branched *N*-alkyl groups turned out to be more able than *anti* complex **10b** to furnish the desired cross-coupling product **37** over the homocoupling product **38**. A peculiar behavior was shown by catalysts **11c** and **12c** possessing an *N*′-mesityl group (entries 7 and 8), for which the relative configuration of phenyls on the NHC backbone strongly differentiates yields of heterocoupled product **37** while giving very similar *E*/*Z* ratios, underlining how catalytic efficiency is influenced by a delicate balance between NHC backbone configuration and steric features of *N*-substituents.

The increasing interest in industrially relevant cross-metathesis reactions such as ethenolysis of fatty acid monoesters derived from renewable biomass to produce higher value-added products[3c,d,f,27] prompted us to investigate the catalytic potential of newly developed systems in the ethenolysis of ethyl oleate (**39**; Scheme 4 and Table 4). Indeed, ruthenium complexes bearing unsymmetrical NHCs have already demonstrated their attractiveness as catalysts for the cross-metathesis of methyl oleate with ethylene, showing high selectivities for ethenolysis products over self-metathesis products.[7d]

This feature was attributed to their strong preference to propagate as a methylidene species.[28]

As reported in Table 4 (entries 1–12), catalysts **9b**, **10b**, **11a–c**, and **12a–c** were all compared at 500 ppm catalyst loading and 10 bar of ethylene (99.9% purity). Data for the same reaction carried out in the presence of **HGII** (entry 10) were added. Moreover, comparison with **BerEt**[29a] catalyst (Figure 8), bearing a cyclic alkylaminocarbene (CAAC) ligand (entry 9), was included, since ruthenium complexes with CAAC ligands are the most active catalysts for ethenolysis known to date.[29b–f]

Scheme 4. Ethenolysis of Ethyl Oleate (39)

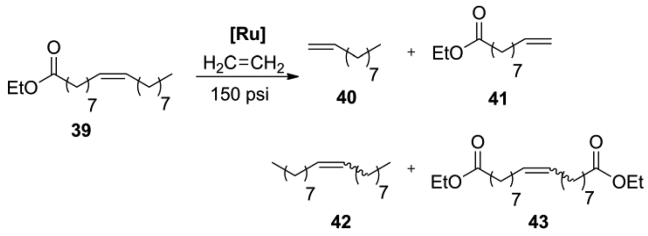

Higher selectivities, yields, and turnover numbers (TONs) were displayed by catalysts with *anti* backbone configuration (Table 4, entries 4, 6, and 8), which gave better performances than symmetrical **HGII** catalyst. *Anti* catalyst **10b**, although it gave an improved yield and TON with respect to its *syn* congener **9b** (cf. entries 1 and 2), showed lower selectivity. On the other hand, catalyst **9b** was already found to show a peculiar behavior, revealing a marked propensity to give nonproductive metathesis events,[13b] which is a desirable feature for targeted reactions such as ethenolysis. The nature of the *N*-alkyl group seems to have a slight effect on the selectivity of ethenolysis reactions (entries 3–6), while the sterics of the *N*-aryl substituent (mesityl versus 2-isopropylphenyl) strongly influences catalyst activity, as was evident, above all, when catalysts **9b** and **10b** were compared with catalysts **11c** and **12c**. Indeed selectivities, yields, and TONs obtained with the latter catalysts nearly equal those found for the high-performing **BerEt** catalyst (entries 7–9). In particular, **12c** showed the same selectivity as **BerEt** (83%).

Encouraged by this finding, as only a few examples of ruthenium complexes with NHC ligands were found to be very efficient in ethenolysis reactions, we tested catalyst **12c** at lower catalyst loadings (Table 4, entries 11–14). Under the same conditions, the superiority of reference **BerEt** catalyst, and more in general of CAAC ruthenium complexes, was already demonstrated.[29b–f] At a catalyst loading of 100 ppm a selectivity of 86% for ethenolysis products **40** and **41** and a TON of 4100 were observed (entry 11). When the reaction time was also reduced (entry 12), 90% selectivity was achieved and yield (44%) and TON (4400) were slightly improved. At 100 ppm, a lower reaction temperature (40 °C) afforded lower yield and TON (entry 13), while at a catalyst loading as low as 20 ppm and 50 °C (entry 14), **12c** displayed unchanged selectivity (83%) and the best TON reported so far for *N*-alkyl/*N*-aryl NHC complexes.[7d]

Asymmetric Metathesis Reactions. The catalytic performances of enantiomerically pure catalysts **12a–c**[30] were also evaluated in asymmetric metathesis transformations and compared to those of catalyst **10b**.[13b] The asymmetric ring-closing metahesis (ARCM) of achiral trienes **44** and **45** (Scheme 5) and the asymmetric ring-opening cross-metathesis (AROCM) of *meso*-norbornene derivative **48** with styrene (Scheme 6) were chosen as model reactions. The results for ARCM reactions are reported in Table 5 and compared to those of catalyst **2a**, representing the closest example of

DOI: 10.1021/acs.organomet.7b00488
Organometallics XXXX, XXX, XXX–XXX

Table 4. Ethenolysis of Ethyl Oleate (39) with Catalysts 9b, 10b, 11a–c, and 12a–c

entry[a]	cat.	cat./39 (ppm)	temp (°C)	time (h)	conversion[b] (%)	selectivity[c] (%)	yield[d] (%)	TON[e]
1	**9b**	500	50	3	38	77	29	580
2	**10b**	500	50	3	63	58	36	720
3	**11a**	500	50	3	53	60	32	640
4	**12a**	500	50	3	70	64	45	900
5	**11b**	500	50	3	53	43	23	460
6	**12b**	500	50	3	71	57	40	800
7	**11c**	500	50	3	75	81	61	1220
8	**12c**	500	50	3	81	83	67	1340
9	**BertEt**	500	50	3	85	83	70	1400
10	**HGII**	500	50	3	71	43	30	600
11	**12c**	100	50	3	48	86	41	4100
12	**12c**	100	50	2	49	90	44	4400
13	**12c**	100	40	3	39	88	34	3400
14	**12c**	20	50	3	18	83	15	7500

[a]The reactions were run neat using 5.4 mmol of ethyl oleate at 150 psi of ethylene (99.9% purity) with dodecane (150 μL) used as an internal standard. [b]Determined by GC analysis. Conversion = 100 − [(final moles of **39**) × 100/[initial moles of **39**]. [c]Determined by GC analysis. Selectivity = 100(moles of ethenolysis products **40** + **41**)/[(moles of **40** + **41**) + (2 × (moles of **42** + **43**))]. [d]Yield= (conversion × selectivity)/100. [e]TON = yield × (initial moles of **39**/moles of catalyst)/100.

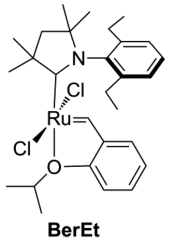

BerEt

Figure 8. Ruthenium complex with a CAAC ligand (Bertrand's catalyst).

Scheme 5. ARCM of 44 and 45

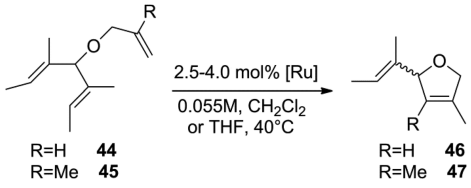

enantioselective catalyst with a monodentate C_1-symmetric NHC ligand.[8a]

With regard to the enantioselective desymmetrization of triene **44** (Table 5), the only discriminating factor for both the yield and for the enantioselectivity appeared to be the nature of the *N*′-aromatic substituent. Indeed, catalysts **12a**,**b** containing an *N*′-2-isopropylphenyl group were able to promote the ARCM of triene **44** in high yields and low enantiomeric

Table 5. ARCM of 44 and 45 with 10b, 12a–c, and 2a

entry[a]	substrate	cat. (mol %)	additive	time (h)	yield[b] (%)	ee[c] (%)
1[d]	44	**10b** (2.5)	none	2	>98	19 (*S*)
2[d]	44	**10b** (4.0)	NaI	2	>95	52 (*S*)
3	44	**12a** (2.5)	none	2	>98	16 (*S*)
4	44	**12a** (4.0)	NaI	2	>98	43 (*S*)
5	44	**12b** (2.5)	none	2	>98	18 (*S*)
6	44	**12b** (4.0)	NaI	2	83	47 (*S*)
7	44	**12b** (4.0)	NaI	20	87	43 (*S*)
8	44	**12c** (2.5)	none	2	18	7 (*R*)
9	44	**12c** (2.5)	none	41	>98	7 (*R*)
10	44	**12c** (4.0)	NaI	2	7	24 (*S*)
11	44	**12c** (4.0)	NaI	25	7	24 (*S*)
12[e]	44	**2a** (2.5)	none	2	>95	82 (S)
13[e]	44	**2a** (4.0)	NaI	2	>95	48 (S)
14[d]	45	**10b** (2.5)	none	3	>95	42 (*S*)
15[d]	45	**10b** (4.0)	NaI	3	-	-
16	45	**12a** (2.5)	none	3	>98	41 (*R*)
17	45	**12a** (4.0)	NaI	3	-	-
18	45	**12b** (2.5)	none	3	>95	36 (*S*)
19	45	**12b** (4.0)	NaI	3	-	-
20	45	**12c** (2.5)	none	3	-	-
21[f]	45	**2a** (2.5)	none		95	8 (S)

[a]Reactions without additive were performed in CH_2Cl_2; reactions with NaI were carried out in THF. Temperature: 40 °C. [b]Yields based on NMR analysis. [c]Enantiomeric excesses determined by chiral GC. [d]Taken from ref 13. [e]Reference 8b. [f]Reference 32.

Scheme 6. AROCM of 48 with Styrene

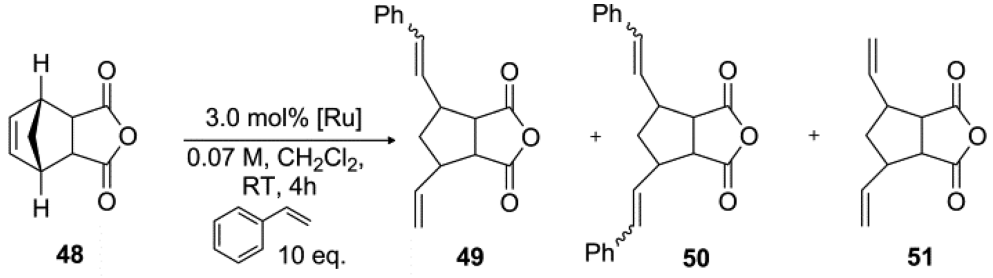

DOI: 10.1021/acs.organomet.7b00488
Organometallics XXXX, XXX, XXX–XXX

excesses, as already observed for the parent catalyst **10b** (entries 1, 3, and 5), whereas complex **12c** with an *N*-mesityl group gave the cyclic product **46** in only 18% yield and 7% ee (entry 8). Prolonged reaction time led to almost quantitative formation of **46** (entry 9), while it did not improve the enantiomeric excess. In an effort to enhance enantioselectivity, as occurred with ARCM reactions promoted by chiral systems based on C_2-symmetric NHCs,[31] the effect of using an additive such as NaI was investigated. A good increase in enantiomeric excesses was found for both **12a** and **12b** (entries 4 and 6), although to a lesser extent than for **10b** (entry 2). Moreover, for **12b** the presence of NaI led to a decrease in the formation of cyclic product **46**, and also a longer reaction time resulted in comparable results in terms of both product yield and enantioselectivity (entries 6 and 7). The addition of NaI to **12c** had a deleterious effect on yield and caused inversion of enantioselectivity (entries 10 and 11).

In analogy with **10b** (Table 5, entry 14), catalysts **12a,b** successfully accomplished the most challenging ARCM of **45** to generate tetrasubstituted olefin **47** in moderate enantiomeric excesses (entries 16 and 18), while **12c** was found to be inactive. Very likely, the bulkiness of the *N*′-mesityl group reduces the active space around the metal, preventing the approach of the sterically encumbered triene **45**.

Attempts to improve reaction enantioselectivity using NaI as an additive failed (Table 5, entries 15, 17, and 19). As a general remark, in both ARCM reactions, catalysts **12a−c** showed behaviors quite different from that of catalyst **2a**.[8a] Indeed, in the ARCM of **44** they disclosed lower enantiomeric excesses and opposite response to the addition of NaI with respect to **2a** (entries 12 and 13). On the other hand, they proved to be much more enantioselective than **2a** in the ARCM of **45** (entry 21).[32]

Concerning the AROCM of *cis*-5-norbornene-*endo*-2,3-dicarboxylic anhydride (**48**) with styrene (Scheme 6), the results are summarized in Table 6. It should be noted that

Table 6. AROCM of 48 with Styrene in the Presence of 10b and 12a−c

entry	catalyst	isolated yield of **49** (%)	isolated yield of **50** (%)	isolated yield of **51** (%)	ee (**49**)[a] (%)
1[b]	**10b**	46	15	10	13
2	**12a**	57	11	16	19
3	**12b**	45	11	16	21
4	**12c**	37	16	22	43

[a]Enantiomeric excess determined by chiral HPLC. [b]Reference 13b.

N,*N*′-diaryl catalysts, such as those reported by Hoveyda, Grubbs, and Blechert,[33] are the most effective catalysts for AROCM reactions known up to now. As the NHC architecture is very different from that of our catalysts, we found more appropriate to refer results reported with the newly synthesized catalysts to those obtained by Grubbs with more similar *N*-alkyl/*N*′-aryl NHC ruthenium metathesis catalysts, showing the highest selectivity at 82% ee.[34]

All of the catalysts promoted AROCM of **48** with conversions >98%, as determined by ^{1}H NMR spectroscopic analysis of crude reaction mixture after 4 h. The desired product **49** was obtained in 37−57% isolated yields, along with the side products **50** and **51** (see Table 6), also obtained in AROCM reactions promoted by Grubbs' *N*-alkyl/*N*′-aryl catalysts.[34] Analogously, no other compound was detected in the reaction mixture, except for stilbene derived from the homometathesis of styrene, and only products having trans stereochemistry were obtained.

Low to moderate enantiomeric excesses were registered, and the highest ee value (43%) was achieved with catalyst **12c**, which also gave a product distribution slightly different from that of the catalysts **10b** and **12a,b** (Table 6, entry 4) suggesting a major propensity of **12c** to propagate via a methylidene species,[28] as observed in ethenolysis reactions.

CONCLUSION

New Hoveyda−-Grubbs catalysts with unsymmetrical NHC ligands combining differently encumbered *N*-substituents and *syn* or *anti* phenyl groups on the backbone (**11a−c**, **12a−c**) have been developed. Their thermal stabilities and their catalytic behaviors were investigated and compared to those of analogous complexes with *N*-cyclohexyl/*N*′-2-isopropylphenyl groups (**9b**, **10b**) as well as to commercially available **HGII** bearing a symmetrical NHC. *N*′-2-Isopropylphenyl complexes with an *anti* backbone (**10b**, **12a−c**) are more stable than their *syn* isomers (**9b**, **11a−c**), and the nature of *N*-alkyl substitution (neopentyl, neophyl vs cyclohexyl) accounts for the observed stability order. *N*′-Mesityl catalysts (**11c**, **12c**) show outstanding stabilities that can be correlated to their higher steric bulkiness. In the RCM reactions of less encumbered substrates, the introduction of bulky, highly branched *N*-alkyl groups leads to reduced activity differences between *syn* and *anti* complexes with respect to complexes with an *N*-cylohexyl group, whereas the presence of an *N*′-mesityl substituent gives rise to lower activities, also correlated to the nature of the NHC backbone configuration. In all cases, catalytic performances are inferior to those of **HGII** catalyst. In the RCM of more demanding substrates, the *N*′-2-isopropylphenyl *anti* catalyst with an *N*-neopentyl substituent (**12a**) is found to be highly efficient, nearly equaling the performance of an analogous catalyst with an *N*-cyclohexyl group (**10b**), while *N*′-mesityl catalysts (**11c**, **12c**) show dramatically lower activities, proving to be less efficient also than **HGII** that, as is well-known, is scarcely competent to promote this class of reactions. On the other hand, catalysts **11c** and **12c** gave interesting results in the ethenolysis of ethyl oleate, outperforming their analogues and **HGII**. In particular, *anti* catalyst **12c** gives up to 90% selectivity for ethenolysis over self-metathesis products with a TON of 4400 and, at low catalyst loading (20 ppm), displays 83% selectivity with a TON of 7500, which is the best result reported to date for ethenolysis reactions promoted by *N*-alkyl/*N*′-aryl NHC ruthenium catalysts. Asymmetric metathesis transformations mediated by enantiopure *anti* catalysts **12a−c** clearly indicate that the nature of the *N*′-aromatic group is the main discriminating factor for the observed activities and enantioselectivities. The strong influence of the type of NHC substitution pattern on metathesis reactions evidenced by this study underlines, once again, the importance of identifying NHC structural modifications that can allow the design of improved active and selective catalysts.

EXPERIMENTAL SECTION

General Information. All reactions involving organometallic compounds were performed under nitrogen using standard Schlenk and glovebox techniques. Diamines **13**,[13a] **17**,[13b] and **18**,[13a] substrates for metathesis reactions,[35] and 2-methyl-2-phenylpropanaldehyde[36] were prepared according to the literature procedures. Ethyl oleate was

DOI: 10.1021/acs.organomet.7b00488
Organometallics XXXX, XXX, XXX−XXX

purchased from Sigma-Aldrich Company and stored on activated neutral alumina before use. All other reagents were purchased from Sigma-Aldrich and TCI Chemicals and used without further purifications. Solvents were dried and distilled before use. Deuterated solvents were degassed under a N_2 flow and stored over activated 4 Å molecular sieves. Flash column chromatography of ligand intermediates was performed using silica gel 60 (230−400 mesh) from Sigma-Aldrich, and flash column chromatography of organometallic compounds was performed, under nitrogen flow, using silica gel 60 (230−400 mesh) from TSI Cambridge. Analytical thin-layer chromatography (TLC) was performed using silica gel 60 F254 precoated plates with a fluorescent indicator. The visualization was performed using UV light or $KMnO_4$. NMR spectra were recorded on a Bruker Avance 250 spectrometer (250 MHz for ^{1}H; 62.5 MHz for ^{13}C), a Bruker AM 300 spectrometer (300 MHz for ^{1}H; 75 MHz for ^{13}C), a Bruker AVANCE 400 spectrometer (400 MHz for ^{1}H; 100 MHz for ^{13}C; 161.97 MHz for ^{31}P), and a Bruker ASCEND 600 spectrometer (600 MHz for ^{1}H; 150 MHz for ^{13}C). NMR samples were prepared by dissolving about 10 mg of compounds in 0.5 mL of deuterated solvent. ^{1}H and ^{13}C chemical shifts are listed in parts per million (ppm) downfield from TMS and are referenced from the solvent peaks or TMS. ^{31}P chemical shifts are referenced using H_3PO_4 as external standard. Spectra are reported as follows: chemical shift (ppm), multiplicity, and integration. Multiplicities are abbreviated as follows: singlet (s), doublet (d), triplet (t), multiplet (m), broad (br), overlapped (o). Elemental analyses for C, H, and N were recorded on a ThermoFinnigan Flash EA 1112 instrument and were performed according to standard microanalytical procedures. Electrochemical measurements were conducted with an AUTOLAB PG STAT 302N potentiostat. A three-electrode configuration was employed. The working electrode was a Pt disk (diameter 2 mm), the counter electrode a Pt bar, and the reference a quasi-reference electrode (PtQRE)1, calibrated vs octamethylferrocene as internal standard. All cyclic voltammograms were recorded in dry CH_2Cl_2 under a nitrogen atmosphere using NBu_4PF_6 (0.1 M) as supporting electrolyte at a scan rate of 100 mV/s. Potentials were referenced against the potential of octamethylferrocene. ESI-MS measurements of organic compounds were performed on a Waters Quattro Micro triple quadrupole mass spectrometer equipped with an electrospray ion source. ESI-FT-ICR measurements of complexes were performed on a Bruker Solaris XR instrument. Enantiomeric excesses were determined by chiral GC (Agilent Technologies 6850) or by chiral HPLC (JASCO MD-4015 Photo diode array detector, PU4180 RMPLC Pump) and were compared to racemic samples. Ethenolysis mixture composition was determined by GC (Agilent Technologies 7890A). Optical activity was determined using a JASCO P2000 polarimeter.

The DFT calculations were performed with the Gaussian09 set of programs,[37] using the BP86 functional of Becke and Perdew.[38] The electronic configuration of the molecular systems was described with the standard split-valence basis set with a polarization function of Ahlrichs and co-workers for H, C, N, O, and Cl (SVP keyword in Gaussian).[39] For Ru we used the small-core, quasi-relativistic Stuttgart/Dresden effective core potential, with an associated (8s7p6d)/[6s5p3d] valence basis set contracted according to a (311111/22111/411) scheme (standard SDD keywords in Gaussian09).[40] The geometry optimizations were performed without symmetry constraints, and the characterization of the located stationary points was performed by analytical frequency calculations.

$\%V_{Bur}$ was calculated by starting from DFT optimized structures by choosing the metal as the center of the sphere, selecting atomic Bondi radii scaled by 1.17 and a radius sphere of 3.5.

Synthesis of 11a−c and 12a−c. *General Procedure for the Arylation of Diamines.* Under a nitrogen atmosphere, in a round-bottom flask equipped with a magnetic stirrer and a condenser, 2,2′-bis(diphenylphosphino)-1,1′-binaphthyl (BINAP) (0.2 equiv), palladium acetate (0.1 equiv), sodium *tert*-butoxide (2 equiv), and toluene (C = 0.05 M) were introduced. The orange solution was stirred for a few minutes. Then the diamine (1 equiv) and mesityl bromide (1 equiv) were added and the reaction mixture was heated to 100 °C for 48 h. After this time the purple mixture was cooled to room temperature, diluted with hexane, and then filtered through a plug of silica gel with methanol as eluent. The crude yellow oil was purified by flash column chromatography on silica gel (hexane/ethyl acetate 9/1 to 6/4) to give the desired product as a yellow oil.

*N^1-Mesityl-1,2-diphenylethane-1,2-diamine (**14**).* MW = 330.5 g/mol. Yield: 79%. ^{1}H NMR (300 MHz, $CDCl_3$): δ 7.29−7.27 (m, 3H, Ar-*H*); 7.23−7.20 (m, 3H, Ar-*H*); 7.10−7.07 (m, 2H, Ar-*H*); 7.02−6.98 (m, 2H, Ar-*H*); 6.75 (s, 2H, Ar-*H*); 4.43 (d, J = 4.9 Hz, 1H, N-C*H*-CH-N); 4.35 (d, J = 5.2 Hz, 1H, N-CH-C*H*-N); 2.21 (s, 3H, Ar-CH_3); 2.16 (s, 6H, Ar-CH_3). ^{13}C{^{1}H} NMR (75 MHz, $CDCl_3$): δ 143.8; 142.8; 139.8; 130.1; 129.7 (overlapped); 128.5; 128.2; 128.1; 127.8; 127.2; 127.1; 67.7; 60.2; 20.6; 19.3. ESI+MS: m/z 353.2 (MNa^+).

*(1R,2R)-N^1-cyclohexyl-N^2-mesityl-1,2-diphenylethane-1,2-diamine (**20**).* MW = 412.6 g/mol. Yield: 51%. ^{1}H NMR (400 MHz, $CDCl_3$): δ7.20−7.15 (m, 5H, Ar-*H*); 7.09 (br s, 3H, Ar-*H*); 7.01−6.99 (m, 2H, Ar-*H*); 6.67 (s, 2H, Ar-*H*); 4.41 (d, J = 7.2 Hz, 1H, N-C*H*-CH-N); 4.21 (d, J = 7.2 Hz, 1H, N-CH-C*H*-N); 2.33−2.28 (m, 1H, Cy-*H*); 2.15 (s, 3H, Ar-CH_3); 2.13 (s, 6H, Ar-CH_3); 2.01−1.98 (br d, 1H, Cy-*H*); 1.67 (br t, 3H, Cy-*H*); 1.54 (br s, 1H, Cy-*H*); 1.17−1.10 (m, 5H, Cy-*H*). ^{13}C{^{1}H} NMR (100 MHz, $CDCl_3$) δ: 142.4; 142.3; 141.9; 129.8; 128.3; 128.0; 127.9 (overlapped); 127.8; 126.9; 67.1; 65.5; 53.7; 35.0; 32.8; 26.3; 25.2, 24.8, 20.5, 19.6. ESI+MS: m/z 413.9 (MH^+). $[\alpha]_D^{20}$ = −45.3° (c = 0.5, CH_2Cl_2).

General Procedure for the Alkylation of Diamines. A round-bottom flask was charged with the diamine (1 equiv), the carbonylic compound (3 equiv of pivalaldehyde for **15a** and **19a**, 6 equiv of 2-methyl-2-phenylpropanaldehyde for **15b** and **19b**, and 7 equiv of cyclohexanone for **15c**) and anhydrous methylene chloride (C = 0.1 M). The reaction mixture was stirred at room temperature over activated molecular sieves 4 Å for 48 h (**15a**), 14 h (**19a**), or 5 days (**15b**, **19b**, and **15c**) and then filtered. Then, the solvent was removed under reduced pressure and anhydrous MeOH was added (C = 0.1 M) followed by portionwise addition of $NaBH_4$ (4 equiv) under a nitrogen atmosphere. The reaction mixture was stirred for 3.5 h, diluted with methylene chloride, and extracted with water. The organic layer was dried over anhydrous Na_2SO_4, and then the solvent was removed under vacuum to afford a yellowish oil which was then purified by flash column chromatography on silica gel (hexane/ethyl acetate 9/1).

*N^1-(2-Isopropylphenyl)-N^2-neopentyl-1,2-diphenylethane-1,2-diamine (**15a**).* MW = 400.6 g/mol. Yield: 60%. ^{1}H NMR (300 MHz, $CDCl_3$): δ 7.31−7.30 (m, 3H, Ar-*H*); 7.25−7.23 (m, 3H, Ar-*H*); 7.19−7.16 (m, 1H, Ar-*H*); 7.08−7.01 (m, 3H, Ar-*H*); 6.91 (t, J = 8.0 Hz, J = 7.2 Hz, 1H, Ar-*H*), 6.68 (t, J = 7.4 Hz, J = 7.4 Hz, 1H, Ar-*H*); 6.31 (d, J = 8.2 Hz, 1H, Ar-*H*); 5.42 (br s, 1H, Ar-*H*); 4.63 (t, J = 4.7 Hz, J = 4.7 Hz, 1H, N-C*H*-CH-N); 4.15 (d, J = 4.7 Hz, 1H, N-CH-C*H*-N); 3.12−2.99 (m, 1H, Ar-C*H*-(CH_3)$_2$); 2.37 (d, J = 11.4 Hz, 1H, N-CH_2-C(CH_3)$_3$); 2.20 (d, J = 11.4 Hz, 1H, N-CH_2-C(CH_3)$_3$); 1.41 (d, J = 6.6 Hz, 3H, Ar-CH-(CH_3)$_2$); 1.35 (d, J = 6.8 Hz, 3H, Ar-CH-(CH_3)$_2$); 0.97 (s, 9H, N-CH$_2$-C(CH_3)$_3$). ^{13}C{^{1}H} NMR (75 MHz, $CDCl_3$) δ: 143.9; 140.2; 139.8; 132.2; 128.2; 128.1; 127.9; 127.8; 127.4; 127.2; 126.6; 124.8; 116.9; 111.7; 68.7; 62.8; 59.8; 31.8; 27.8; 27.7; 22.5; 22.4. ESI+MS: m/z 401.4 (MH^+).

*(1R,2R)-N^1-(2-Isopropylphenyl)-N^2-neopentyl-1,2-diphenylethane-1,2-diamine (**19a**).* MW = 400.6 g/mol. Yield: 70%. ^{1}H NMR (300 MHz, CD_2Cl_2): δ 7.33−7.22 (m, 10H, Ar-*H*); 7.15 (dd, J = 7.7 Hz, J = 1.3 Hz, 1H, Ar-*H*); 6.83 (dt, J = 7.6 Hz, J = 1.5 Hz, 1H, Ar-*H*); 6.64 (dt, J = 7.0 Hz, 1H, Ar-*H*); 6.21 (d, J = 8.1 Hz, 1H, Ar-*H*); 5.82 (br s, 1H, N*H*); 4.42 (d, J = 6.9 Hz, 1H, N-C*H*-CH-N); 3.86 (d, J = 6.8 Hz, 1H, N-CH-C*H*-N); 3.25−3.16 (m, 1H, Ar-C*H*-(CH_3)$_2$); 2.28 (d, J = 11.3 Hz, 1H,, N-CH_2-C(CH_3)$_3$); 2.09 (d, J = 11.3 Hz, 1H,, N-CH_2-C(CH_3)$_3$); 1.42 (d, J = 6.8 Hz, 3H, Ar-CH-(CH_3)$_2$); 1.38 (d, J = 6.7 Hz, 3H, Ar-CH-(CH_3)$_2$); 0.95 (s, 9H, N-CH$_2$-C(CH_3)$_3$). ^{13}C{^{1}H} NMR (75 MHz, CD_2Cl_2) δ: 144.7; 142.4; 141.7; 133.2; 128.6; 128.5; 128.1; 127.5; 127.3; 126.5; 125.0; 117.2; 111.9; 70.4; 64.4; 60.1; 31.8; 27.8; 27.7; 23.0; 22.4. ESI+MS: m/z 401.4 (MH^+). $[\alpha]_D^{20}$ = +49.1 (c = 0.5, CH_2Cl_2).

*N^1-(2-Isopropylphenyl)-N^2-(2-methyl-2-phenylpropyl)-1,2-diphenylethane-1,2-diamine (**15b**).* MW = 462.7 g/mol. Yield: 73%. ^{1}H NMR (250 MHz, $CDCl_3$): δ 7.28 (d, J = 4.4 Hz, 4H, Ar-*H*); 7.21−

DOI: 10.1021/acs.organomet.7b00488
Organometallics XXXX, XXX, XXX−XXX

7.20 (m, 4H, Ar-*H*); 7.09−7.07 (m, 4H, Ar-*H*);6.86 (d, *J* = 7.3 Hz, 2H, Ar-*H*); 6.82−6.77 (m, 3H, Ar-*H*); 6.60 (t, *J* = 7.5 Hz, *J* = 7.3 Hz, 1H, Ar-*H*); 6.19 (d, *J* = 7.9 Hz, 1H, Ar-*H*); 5.12 (d, *J* = 5.1 Hz, 1H, N*H*); 4.43 (t, *J* = 5.2 Hz, *J* = 5.1 Hz, 1H, N-C*H*-CH-N); 3.99 (d, *J* = 4.9 Hz, 1H N-CH-C*H*-N); 2.90−2.82 (m, 1H, Ar-C*H*-$(CH_3)_2$); 2.62 (d, *J* = 11.3 Hz, 1H, N-CH_2-CPh$(CH_3)_2$); 2.51 (d, *J* = 11.3 Hz, 1H, N-CH_2-CPh$(CH_3)_2$); 1.37 (s, 3H, N-CH_2-CPh$(CH_3)_2$); 1.31−1.29 (m, 6H, N-CH_2-CPh$(CH_3)_2$ and Ar-CH-$(CH_3)_2$); 1.24−1.22 (d, *J* = 6.8 Hz, 3H, Ar-CH-$(CH_3)_2$). $^{13}C\{^1H\}$ NMR (100 MHz, $CDCl_3$) *δ:* 147.7; 143.8; 140.0; 139.7; 132.2; 128.3; 128.1; 128.0; 127.9; 127.7; 127.5; 127.1; 126.5; 126.0; 125.9; 124.7; 116.9; 111.7; 68.4; 62.8; 59.8; 38.9; 27.6; 27.4; 27.0; 22.5; 22.3. ESI+MS: *m/z* 463.2 (MH^+).

(1R,2R)-N¹-(2-Isopropylphenyl)-N²-(2-methyl-2-phenylpropyl)-1,2-diphenylethane-1,2-diamine (**19b**). MW = 462.7 g/mol. Yield: 79%. ^1H NMR (300 MHz, $CDCl_3$): *δ*7.32−7.26 (m, 8H, Ar-*H*); 7.17−7.16 (m 8H, Ar-*H*); 6.83 (br t, 1H, Ar-*H*); 6.64 (br t, 1H, Ar-*H*); 6.14 (d, *J* = 7.6 Hz, 1H, Ar-*H*); 5.61 (br s, 1H, N*H*); 4.24 (br s, 1H, N-C*H*-CH-N); 3.76 (br d, 1H, N-CH-C*H*-N); 3.05 (br t, 1H, Ar-C*H*-$(CH_3)_2$); 2.64 (d, *J* = 10.9 Hz, 1H, N-CH_2-CPh$(CH_3)_2$); 2.48 (d, *J* = 10.9 Hz, 1H, N-CH_2-CPh$(CH_3)_2$); 1.41−1.33 (m, 12H, N-CH_2-CPh$(CH_3)_2$ and Ar-CH-$(CH_3)_2$). $^{13}C\{^1H\}$ NMR (75 MHz, $CDCl_3$) *δ:*147.4; 144.3; 141.8; 141.1; 132.7; 128.4; 128.2; 127.7; 127.3; 127.0; 126.4; 126.0; 124.7; 116.9; 111.7; 69.7; 64.2; 59.8; 38.8; 27.7; 27.6; 27.1; 22.8; 22.4. ESI+MS: *m/z* 463.1 (MH^+). $[\alpha]_D^{20}$ = +65.8 (*c* = 0.5, CH_2Cl_2).

N¹-Cyclohexyl-N²-mesityl-1,2-diphenylethane-1,2-diamine (**15c**). MW = 412.6 g/mol. Yield: 50%. ^1H NMR (300 MHz, $CDCl_3$): *δ* 7.26−7.25 (m, 3H, Ar-*H*); 7.16−7.13 (m, 3H, Ar-*H*); 6.93−6.90 (m, 2H, Ar-*H*); 6.85−6.82 (m, 2H, Ar-*H*); 6.71 (s, 2H, Ar-*H*); 4.91 (br s, 1H, N*H*); 4.49 (br s, 1H, N-C*H*-CH-N); 4.38 (d, *J* = 4.5 Hz, 1H, N-CH-C*H*-N); 2.33 (br s, 1H, Cy-*H*); 2.18 (br s, 9H, Ar-CH_3); 1.99 (br s, 1H, Cy-*H*); 1.71−1.57 (m, 4H, Cy-*H*); 1.38 (br s, 1H, Cy-*H*); 1.18−1.13 (m, 5H, Cy-*H*). $^{13}C\{^1H\}$ NMR (75 MHz, $CDCl_3$) *δ:* 142.8; 141.5; 139.7; 129.7; 129.1; 128.4; 128.0; 127.8; 127.5; 127.1; 127.0; 126.9; 66.8; 63.7; 53.2; 35.1; 33.0; 26.3; 25.1; 24.7; 20.5; 19.8. ESI +MS: *m/z* 413.2 (MH^+).

General Procedure for the Synthesis of Tetrafluoroborate Salts. Diamine (1 equiv) and triethyl orthoformate (8 equiv) were introduced in a flask equipped with a magnetic stirrer and a condenser. The reaction mixture was stirred at room temperature for a few minutes. Then ammonium tetrafluoroborate (1.2 equiv) was added and the solution was heated at 130 °C for 2 h (**16a**, **21a**, **16c**, **22**) or 8 h (**16b**, **21b**). After that, the condenser was removed in order to facilitate evaporation of ethanol produced during the reaction. The crude brownish oil was washed with diethyl ether and purified by flash column chromatography on silica gel (hexane/ethyl acetate 9/1 to 1/1) to obtain the product as a white solid.

3-(2-Isopropylphenyl)-1-neopentyl-4,5-diphenyl-4,5-dihydro-1H-imidazol-3-ium Tetrafluoroborate (**16a**). MW = 498.4 g/mol. Yield: 81%. ^1H NMR (400 MHz, CD_2Cl_2): *δ* 8.70 (s, 1H, N-C*H*-N); 7.50−7.48 (m, 1H, Ar-*H*); 7.36−7.35 (m, 2H, Ar-*H*); 7.25−7.18 (m, 4H, Ar-*H*); 7.11−6.97 (m, 7H, Ar-*H*); 6.19 (br t, 1H, N-C*H*-CH-N); 5.98 (br t, 1H, N-CH-C*H*-N); 4.01 (d, *J* = 14.2 Hz, 1H, N-CH_2-C$(CH_3)_3$); 3.21−3.11 (m, 2H, N-CH_2-C$(CH_3)_3$ and Ar-C*H*-$(CH_3)_2$); 1.34−1.29 (m, 6H, Ar-CH-$(CH_3)_2$); 1.08 (s, 9H, N-CH_2-C$(CH_3)_3$). $^{13}C\{^1H\}$ NMR (100 MHz, CD_2Cl_2): *δ*160.6; 145.6; 131.8; 130.9; 130.5; 130.4; 129.8; 129.5; 129.4; 128.8; 128.7; 127.9; 127.7; 73.6; 72.2; 58.7; 33.2; 29.0; 27.7; 24.5; 24.1. ESI+MS: *m/z* 411.4 ($M - BF_4^-$).

(4R,5R)-3-(2-Isopropylphenyl)-1-neopentyl-4,5-diphenyl-4,5-dihydro-1H-imidazol-3-ium Tetrafluoroborate (**21a**). MW = 498.4 g/mol. Yield: 90%. ^1H NMR (400 MHz, CD_2Cl_2): *δ* 8.58 (s, 1H, N-C*H*-N); 7.58−7.56 (m, 3H, Ar-*H*); 7.45−7.34 (m, 7H, Ar-*H*); 7.27−7.25 (m, 2H, Ar-*H*); 7.21−7.18 (m, 2H, Ar-*H*); 5.53 (d, *J* = 8.0 Hz, 1H, N-C*H*-CH-N); 5.37 (d, *J* = 8.0 Hz, 1H, N-CH-C*H*-N); 3.82 (d, *J* = 14.9 Hz, 1H, N-CH_2-C$(CH_3)_3$); 3.06 (d, *J* = 14.9 Hz, 1H, N-CH_2-C$(CH_3)_3$)); 2.96−2.89 (m, 1H, Ar-C*H*-$(CH_3)_2$); 1.23 (d, *J* = 6.8 Hz, 3H, Ar-CH-$(CH_3)_2$); 1.09 (s, 9H, N-CH_2-C$(CH_3)_3$); 1.02 (d, *J* = 6.8 Hz, 3H, Ar-CH-$(CH_3)_2$). $^{13}C\{^1H\}$ NMR (100 MHz, CD_2Cl_2): *δ* 159.3; 145.9; 135.1; 134.7; 131.4; 131.0; 130.9; 130.8; 130.7; 130.3; 130.2; 128.8; 128.0; 127.9; 127.7; 127.6; 127.5; 127.0; 78.1; 75.4; 57.6; 33.6; 28.7; 28.0; 24.5; 23.8. ESI+MS: *m/z* 411.5 ($M - BF_4^-$).

$[\alpha]_D^{20}$ = +313.0 (*c* = 0.5, CH_2Cl_2).

3-(2-Isopropylphenyl)-1-(2-methyl-2-phenylpropyl)-4,5-diphenyl-4,5-dihydro-1H-imidazol-3-ium Tetrafluoroborate (**16b**). MW = 560.5 g/mol. Yield: 71%. ^1H NMR (400 MHz, CD_2Cl_2): *δ* 8.36 (s, 1H, N-C*H*-N); 7.41−7.32 (m, 9H, Ar-*H*); 7.20−7.19 (m, 4H, Ar-*H*); 7.00−6.98 (m, 3H, Ar-*H*); 6.83 (d, *J* = 6.8 Hz, 3H, Ar-*H*); 5.73 (d, *J* = 12.4 Hz, 1H, N-C*H*-CH-N); 4.91 (d, *J* = 11.6 Hz, 1H, N-CH-C*H*-N); 4.33 (d, *J* = 14.4 Hz, 1H, N-CH_2-CPh$(CH_3)_2$); 3.57 (d, *J* = 14.4 Hz, 1H, N-CH_2-CPh$(CH_3)_2$); 3.02−2.92 (m, 1H, Ar-C*H*-$(CH_3)_2$); 1.54 (s, 3H, N-CH_2-CPh$(CH_3)_2$); 1.45 (s, 3H, N-CH_2-CPh$(CH_3)_2$); 1.29−1.27 (m, 6H, Ar-CH-$(CH_3)_2$). $^{13}C\{^1H\}$ NMR (100 MHz, CD_2Cl_2): *δ* 160.1; 145.4; 145.2; 131.6; 130.9; 130.2; 129.6; 129.5; 129.2; 128.6; 127.8; 127.6; 126.4; 73.3; 71.1; 59.1; 39.8; 28.9; 27.7; 25.6; 24.5; 24.1. ESI+MS: *m/z* 474.9 ($M - BF_4^-$).

(4R,5R)-3-(2-Isopropylphenyl)-1-(2-methyl-2-phenylpropyl)-4,5-diphenyl-4,5-dihydro-1H-imidazol-3-ium Tetrafluoroborate (**21b**). MW = 560.5 g/mol. Yield: 90%. ^1H NMR (300 MHz, $CDCl_3$): *δ* 8.46 (s, 1H, N-C*H*-N); 7.50−7.45 (m, 7H, Ar-*H*); 7.37−7.09 (m, 9H, Ar-*H*); 6.97 (d, *J* = 8.3 Hz, 1H, Ar-*H*); 6.81 (d, *J* = 7.6 Hz, 2H, Ar-*H*); 5.00 (d, *J* = 8.3 Hz, 1H, N-C*H*-CH-N); 4.60 (d, *J* = 8.0 Hz, 1H, N-CH-C*H*-N); 4.30 (d, *J* = 14.8 Hz, 1H, N-CH_2-CPh$(CH_3)_2$); 3.55 (d, *J* = 14.8 Hz, 1H, N-CH_2-CPh$(CH_3)_2$); 2.67−2.56 (m, 1H, Ar-C*H*-$(CH_3)_2$); 1.57 (s, 3H, N-CH_2-CPh$(CH_3)_2$); 1.40 (s, 3H, N-CH_2-CPh$(CH_3)_2$); 1.15 (d, *J* = 6.7 Hz, 3H, Ar-CH-$(CH_3)_2$); 0.86 (d, *J* = 6.9 Hz, 3H, Ar-CH-$(CH_3)_2$). $^{13}C\{^1H\}$ NMR (100 MHz, CD_2Cl_2): *δ* 158.9; 145.5; 145.2; 134.9; 134.2; 130.9; 130.7; 130.4; 130.3; 129.6; 129.3; 127.9; 127.5; 127.4; 127.2; 126.8; 126.5; 73.6; 57.7; 39.6; 28.4; 28.2; 25.9; 24.7; 23.6. ESI+MS: *m/z* 474.9 ($M - BF_4^-$). $[\alpha]_D^{20}$ = +210.6 (*c* = 0.5, CH_2Cl_2).

1-Cyclohexyl-3-mesityl-4,5-diphenyl-4,5-dihydro-1H-imidazol-3-ium Tetrafluoroborate (**16c**). MW = 510.4 g/mol. Yield: 79%. ^1H NMR (300 MHz, $CDCl_3$): *δ* 8.45 (s, 1H, N-C*H*-N); 7.24−7.23 (m, 4H, Ar-*H*); 7.03−6.92 (m, 4H, Ar-*H*); 6.85−6.72 (m, 4H, Ar-*H*); 6.61 (d, *J* = 11.8 Hz, 1H, N-C*H*-CH-N); 5.95 (d, *J* = 11.8 Hz, 1H, N-CH-C*H*-N); 3.63 (t, 1H, Cy-*H*); 2.48 (s, 3H, Ar-CH_3); 2.33−2.20 (s, 3H, Ar-CH_3); 2.17 (s, 3H, Ar-CH_3); 1.94−1.77 (m, 3H, Cy-*H*); 1.63−1.55 (m, 3H, Cy-H); 1.38−1.21 (m, 3H, Cy-*H*). $^{13}C\{^1H\}$ NMR (100 MHz, $CDCl_3$) *δ:* 157.4; 139.4; 135.2; 133.9; 131.9; 131.1; 130.3; 129.9; 129.3; 129.0; 128.9; 128.2; 127.5; 72.6; 67.8; 58.6; 32.3; 31.8; 25.3; 25.0; 24.9; 20.9; 19.7; 19.5. ESI+MS: *m/z* 425.2 ($M - BF_4^-$).

(4R,5R)-1-Cyclohexyl-3-mesityl-4,5-diphenyl-4,5-dihydro-1H-imidazol-3-ium Tetrafluoroborate (**22**). MW = 510.4 g/mol. Yield: 75%. ^1H NMR (250 MHz, $CDCl_3$) *δ:*8.62 (s, 1H, N-C*H*-N); 7.52−7.32 (m, 7H, Ar-*H*); 7.18−7.15 (m, 3H, Ar-*H*); 6.86 (br s, 1H, Ar-*H*); 6.69 (br s, 1H, Ar-*H*); 5.66 (d, *J* = 8.1 Hz, 1H, N-C*H*-CH-N); 5.12 (d, *J* = 7.9 Hz, 1H,, N-CH-C*H*-N); 3.75−3.66 (br t, 1H, Cy-*H*); 2.35 (s, 3H, Ar-CH_3); 2.19−2.11 (m, 5H, Cy-*H*); 1.92−1.84 (m, 1H, Cy-*H*); 1.75 (s, 3H, Ar-CH_3); 1.63 (s, 3H, Ar-CH_3); 1.45−1.20 (m, 4H, Cy-*H*). $^{13}C\{^1H\}$ NMR (100 MHz, $CDCl_3$): *δ* 156.8; 140.2; 136.3; 134.8; 133.7; 130.7; 130.3; 130.2; 129.5; 129.0; 128.6; 127.0; 75.6; 70.4; 58.5; 32.3; 31.5; 25.1; 24.8; 21.0; 18.8; 18.0. ESI+MS: *m/z* 424.5 ($M - BF_4^-$). $[\alpha]_D^{20}$ = +309.8 (*c* = 0.5, CH_2Cl_2).

General Procedure for the Synthesis of Catalysts. In a glovebox, potassium hexafluoro-*tert*-butoxide (1 equiv) was added to a suspension of tetrafluoroborate salt (1 equiv) in toluene (*C* = 0.1 M). The reaction mixture was stirred for a few minutes at room temperature, and then $(PCy_3)Ru(=CH\text{-}o\text{-}OiPrC_6H_4)Cl_2$ (0.5 equiv) was added. The flask was removed from the glovebox and stirred at 65 °C for 2.0 h. The reaction mixture was cooled to room temperature and purified by flash column chromatography on silica gel (hexane/diethyl ether 5/1 to 1/1).

[3-(2-Isopropylphenyl)-1-neopentyl-4,5-diphenylimidazolidinylidene]dichloro(2-isopropoxyphenylmethylene)ruthenium (**11a**). MW = 730.8 g/mol. Yield: 45%. ^1H NMR (600 MHz, C_6D_6): *δ* 16.29 (major isomer, s, 1H, Ru=C*H*-*o*OiPrC$_6$H$_4$); 16.22 (minor isomer, s, 0.3H); (mixed signals of both isomers) 8.96 (d, *J* = 7.3 Hz, 1H, Ar-*H*); 7.99 (br s, 1H, Ar-*H*); 7.94 (br s, 1H, Ar-*H*); 7.85 (d, *J* = 6.8 Hz, 1H, Ar-*H*); 7.20 (d. *J* = 7.8 Hz, 1H, Ar-*H*); 7.53−7.50 (m, 3H,

DOI: 10.1021/acs.organomet.7b00488
Organometallics XXXX, XXX, XXX−XXX

Ar-*H*); 7.37 (br t, 1H, Ar-*H*); 7.31−7.28 (m, 1H, Ar-*H*); 7.25−7.23 (br t, 1H, Ar-*H*); 7.09−7.03 (m, 3H, Ar-*H*); 6.98 (br s, 3H, Ar-*H*); 6.93−6.90 (m, 1H, Ar-*H*); 6.82−6.65 (m, 5H, Ar-*H*); 6.48 (d, *J* = 9.1 Hz, 1H, Ar-*H*); 6.22 (d, *J* = 7.3 Hz, 1H, Ar-*H*) (only major isomer signals are shown below) 5.99 (t, *J* = 10.0 Hz, 1H, N-C*H*-CH-N); 5.56 (d, *J* = 14.6 Hz, 1H, N-CH_2-(CH_3)$_3$); 5.41 (d, *J* = 10.0 Hz, 1H, N-C*H*-CH-N); 4.70 (br s, 1H, O-C*H*-(CH_3)$_2$); 4.13 (d, *J* = 13.7 Hz, 1H, N-CH_2-(CH_3)$_3$); 3.41 (m, 1H, Ar-C*H*(CH_3)$_2$); 1.77 (s, 6H, O-CH-(CH_3)$_2$); 1.24 (s, 9H, N-CH_2-(CH_3)$_3$); 1.18 (br s, 6H, Ar-CH(CH_3)$_2$). $^{13}C\{^1H\}$ NMR (125 MHz, C_6D_6): δ (only major isomer signals are shown below) 291.8 (Ru=CH-*o*OiPrC_6H_4); 291.2; 216.1; 163.7; 163.5; 153.2; 149.1; 148.9; 148.4; 147.3; 144.5; 143.5; 142.4; 141.3; 139.7; 139.2; 138.9; 138.5; 133.8; 133.3; 133.2; 131.2; 130.7; 130.5; 130.4; 130.2; 129.6; 129.4; 129.3; 129.3; 129.0; 128.9; 128.8; 127.7; 128.6; 127.5; 127.2; 127.0; 126.9; 126.8; 126.1; 122.5; 113.2; 78.3; 77.4; 75.5; 75.2; 70.8; 69.8; 68.6; 65.2; 62.5; 62.0; 61.1; 60.2; 59.8; 32.8; 32.7; 31.3; 30.2; 29.4; 29.3; 29.2; 28.8; 27.7; 27.6; 27.3; 25.6; 24.8; 24.5; 24.4; 24.3; 24.2; 23.6; 22.8; 22.2; 22.1. Anal. Calcd for $C_{39}H_{46}Cl_2N_2ORu$ (730.77): C, 64.10; H, 6.34; N, 3.83. Found: C, 63.88; H, 6.37; N, 3.71. ESI-FT-ICR (**11a**-Cl): *m*/*z* calcd 695.2342, found 695.2339.

*[(4R,5R)-3-(2-Isopropylphenyl)-1-neopentyl-4,5-diphenylimidazolidinylidene]dichloro(2-isopropoxyphenylmethylene)ruthenium (**12a**).* MW = 730.8 g/mol. Yield: 70%. ^1H NMR (600 MHz, C_6D_6): δ 16.38 (minor isomer, s, 0.1H, Ru=CH-*o*OiPrC_6H_4); 16.38 (major isomer, s, 1H); (only major isomer signals are shown below) 7.75 (br s, 2H, Ar-*H*); 7.56 (d, *J* = 6.8 Hz, 2H, Ar-*H*); 7.43 (d. *J* = 8.1 Hz, 1H, Ar-*H*); 7.30 (t, *J* = 7.5 Hz, *J* = 7.5 Hz, 2H, Ar-*H*); 7.19−7.08 (m, 5H, Ar-*H*); 7.02−6.98 (m, 3H, Ar-*H*); 6.67 (t, *J* = 7.4 Hz, *J* = 7.4 Hz, 1H, Ar-*H*); 6.57 (t, *J* = 7.4 Hz, *J* = 7.4 Hz, 1H, Ar-*H*); 6.47 (d, *J* = 8.3 Hz, 1H, Ar-*H*); 5.42 (d, *J* = 13.5 Hz, 1H, N-CH_2-(CH_3)$_3$); 5.26 (d, *J* = 2.7 Hz, 1H, N-C*H*-CH-N); 4.86 (d, *J* = 2.7 Hz, 1H, N-C*H*-CH-N); 4.71−4.67 (m, 1H, O-C*H*-(CH_3)$_2$); 4.16 (d, *J* = 14.8 Hz, 1H, N-CH_2-(CH_3)$_3$); 3.47−3.43 (m, 1H, Ar-C*H*(CH_3)$_2$); 1.78 (d, *J* = 6.0 Hz, 3H, O-CH-(CH_3)$_2$); 1.72 (d, *J* = 6.0 Hz, 3H, O-CH-(CH_3)$_2$); 1.28 (d, *J* = 7.0 Hz, 3H, Ar-CH(CH_3)$_2$); 1.10 (s, 9H, N-CH_2-(CH_3)$_3$); 0.97 (d, *J* = 7.0 Hz, 3H, Ar-CH(CH_3)$_2$). $^{13}C\{^1H\}$ NMR (125 MHz, C_6D_6): δ (only major isomer signals are shown below) 291.7 (Ru=CH-*o*OiPrC_6H_4); 214.4; 153.6; 148.5; 144.7; 140.3; 139.6; 139.4; 133.3; 129.9; 129.7; 129.6; 129.5; 129.4; 129.0; 127.3; 127.2; 127.1; 122.8; 122.6; 113.5; 80.7; 75.4; 73.9; 63.3; 63.2; 33.9; 32.2; 29.8; 28.0; 27.9; 24.9; 24.8; 23.8; 23.7; 23.3; 22.6; 22.6; 22.4; 14.7; 14.5. Anal. Calcd for $C_{39}H_{46}Cl_2N_2ORu$ (730.77): C, 64.10; H, 6.34; N, 3.83. Found: C, 64.12; H, 6.31; N, 3.76. ESI-FT-ICR (**12a**-Cl): *m*/*z* calcd 695.2342, found 695.2344.

*[3-(2-Isopropylphenyl)-1-(2-methyl-2-phenylpropyl)-4,5-diphenylimidazolidinylidene]dichloro(2-isopropoxyphenylmethylene)ruthenium (**11b**).* MW = 792.8 g/mol. Yield: 70%. ^1H NMR (600 MHz, C_6D_6): δ 16.31 (major isomer, s, 1H, Ru=CH-oOiPrC_6H_4); 16.36 (minor isomer, s, 0.2H); (only major isomer signals are shown below) 8.88 (d, *J* = 8.3 Hz, 1H, Ar-*H*); 7.50−7.47 (m, 2H, Ar-*H*); 7.28−7.23 (m, 1H, Ar-*H*); 7.18−7.17 (m, 1H, Ar-*H*); 7.09−7.03 (m, 3H, Ar-*H*); 7.01−6.95 (m, 4H, Ar-*H*); 6.93−6.91 (m, 1H, Ar-*H*); 6.86−6.85 (m, 3H, Ar-*H*); 6.73−6.67 (m, 1H, Ar-*H*); 6.59−6.56 (m, 5H, Ar-*H*); 6.50 (d, *J* = 8.5 Hz, 1H, Ar-*H*); 6.47−6.44 (m, 1H, Ar-*H*); 5.90 (d, *J* = 9.7 Hz, 1H, N-CH_2-(CH_3)$_3$); 5.82 (d, *J* = 13.6 Hz, 1H, N-C*H*-CH-N); 4.91 (d, *J* = 9.7 Hz, 1H, N-CH_2-(CH_3)$_3$); 4.80 (d, *J* = 13.6 Hz, 1H, N-CH-C*H*-N); 4.75−4.71 (m, 1H, O-C*H*-(CH_3)$_2$); 3.42−3.38 (m, 1H, Ar-C*H*(CH_3)$_2$); 2.09 (s, 3H, N-CH_2-CPh(CH_3)$_2$); 1.82−1.80 (m, 6H, O-CH-(CH_3)$_2$); 1.45 (s, 3H, N-CH_2-CPh(CH_3)$_2$); 1.20 (d, *J* = 7.2 Hz, 3H, Ar-CH(CH_3)$_2$); 1.15 (d, *J* = 7.2 Hz, 3H, Ar-CH(CH_3)$_2$). $^{13}C\{^1H\}$ NMR (125 MHz, C_6D_6): δ (mixed signals of both isomers) 292.1; 291.6; 220.6; 215.9; 163.9; 163.7; 153.6; 149.1; 148.5; 148.3; 144.8; 144.5; 141.7; 139.5; 134.1; 133.4; 133.2; 131.4; 130.5; 130.2; 129.8; 129.7; 129.5; 129.3; 129.1; 129.0; 128.8; 128.0; 127.9; 127.9; 127.7; 127.5; 127.1; 127.0; 126.3; 126.3; 126.2; 122.8; 113.5; 78.6; 77.5; 77.4; 75.8; 75.5; 75.4; 70.2; 69.1; 68.7; 65.2; 62.7; 62.2; 61.2; 60.5; 60.1; 39.6; 39.5; 38.9; 34.0; 32.0; 30.5; 29.1; 29.0; 28.6; 28.5; 27.9; 24.8; 24.6; 24.5; 24.5; 24.4; 22.6; 22.5. Anal. Calcd for $C_{44}H_{48}Cl_2N_2ORu$ (792.84): C, 66.66; H, 6.10; N, 3.53. Found: C, 66.70; H, 6.07; N, 3.45. ESI-FT-ICR (**11b**-Cl): *m*/*z* calcd 757.2499, found 757.2494.

*[(4R,5R)-3-(2-Isopropylphenyl)-1-(2-methyl-2-phenylpropyl)-4,5-diphenylimidazolidinylidene]dichloro(2-isopropoxyphenylmethylene)ruthenium (**12b**).* MW = 792.8 g/mol. Yield: 61%. ^1H NMR (600 MHz, C_6D_6): δ 16.39 (minor isomer, s, 0.1H, Ru=CH-oOiPrC_6H_4); 16.36 (major isomer, s, 1H); (only major isomer signals are shown below) 7.50 (d, *J* = 7.6 Hz, 4H, Ar-*H*); 7.19−7.15 (m, 5H, Ar-*H*); 7.11−7.08 (m, 3H, Ar-*H*); 7.02−6.98 (m, 3H, Ar-*H*); 6.91 (d, *J* = 8.1 Hz, 2H, Ar-*H*); 6.84 (t, *J* = 7.6 Hz, *J* = 7.1 Hz, 1H, Ar-*H*); 6.75 (t, *J* = 7.6 Hz, 2H, Ar-*H*); 6.68 (t, *J* = 7.6 Hz, *J* = 7.1 Hz, 1H, Ar-*H*); 6.50 (d, *J* = 8.1 Hz, 1H, Ar-*H*); 5.64 (d, *J* = 14.2 Hz, 1H, N-CH_2-(CH_3)$_3$); 4.79 (d, *J* = 14.2 Hz, 1H, N-CH_2-(CH_3)$_3$); 4.74−4.71 (m, 1H, O-C*H*-(CH_3)$_2$); 4.70 (d, *J* = 1.9 Hz, 1H, N-C*H*-CH-N); 4.60 (d, *J* = 1.9 Hz, 1H, N-CH-C*H*-N); 3.36−3.31 (m, 1H, Ar-C*H*(CH_3)$_2$); 2.06 (s, 3H, N-CH_2-CPh(CH_3)$_2$); 1.82 (d, *J* = 6.2 Hz, 3H, O-CH-(CH_3)$_2$); 1.78 (d, *J* = 6.2 Hz, 3H, O-CH-(CH_3)$_2$); 1.41 (s, 3H, N-CH_2-CPh(CH_3)$_2$); 1.27 (d, *J* = 6.6 Hz, 3H, Ar-CH(CH_3)$_2$); 0.89 (d, *J* = 6.6 Hz, 3H, Ar-CH(CH_3)$_2$). $^{13}C\{^1H\}$ NMR (125 MHz, C_6D_6): δ (only major isomer signals are shown below) 291.6 (Ru=CH-oOiPrC_6H_4); 213.8; 153.6; 148.5; 147.7; 144.7; 139.8; 139.7; 139.5; 133.2; 129.6; 129.5; 129.5; 129.3; 129.2; 127.9; 127.3; 127.1; 126.5; 126.4; 126.2; 122.9; 122.6; 113.5; 80.4; 75.5; 72.8; 63.4; 40.0; 32.3; 32.2; 27.9; 27.8; 25.7; 24.9; 24.8; 23.6; 23.4; 22.6; 22.6; 22.5; 22.4. Anal. Calcd for $C_{44}H_{48}Cl_2N_2ORu$ (792.84): C, 66.66; H, 6.10; N, 3.53. Found: C, 66.69; H, 6.14; N, 3.44. ESI-FT-ICR (**12b**-Cl): *m*/*z* calcd 757.2499, found 757.2505.

*[1-Cyclohexyl-3-mesityl-4,5-diphenylimidazolidinylidene]-dichloro(2-isopropoxyphenylmethylene)ruthenium (**11c**).* MW = 742.8 g/mol. Yield: 63%. ^1H NMR (600 MHz, C_6D_6): δ 16.56 (major isomer, s, 1H, Ru=CH-*o*OiPrC_6H_4); 16.44 (minor isomer, s, 0.1H); 8.78 (br s, 1H, Ar-*H*); 7.37 (br s, 1H, Ar-*H*); 7.15−7.12 (m, 2H, Ar-*H*); 7.00 (t, *J* = 7.5 Hz, *J* = 7.5 Hz, 1H); 6.78 (br s, 1H, Ar-*H*); 6.70−6.67 (m, 5H, Ar-*H*); 6.62−6.60 (m, 3H, Ar-*H*); 6.56 (br s, 1H, Ar-*H*); 6.47 (d, *J* = 8.3 Hz, 1H, Ar-*H*); 6.27 (br s, 1H, Ar-*H*); (only major isomer signals are shown below) 6.04 (d, *J* = 9.3 Hz, 1H, N-C*H*-CH-N); 5.72 (t t, *J* = 3.1 Hz, *J* = 3.4 Hz, 1H, O-C*H*-(CH_3)$_2$); 5.04 (d, *J* = 9.0 Hz, 1H, N-CH-C*H*-N); 4.73−4.68 (m, 1H, Cy-*H*); 3.07 (d, *J* = 11.5 Hz, 1H, Cy-*H*); 2.86 (d, *J* = 12.4 Hz, 1H, Cy-*H*); 2.63 (s, 3H, Ar-CH_3); 2.43 (s, 3H, Ar-CH_3); 1.95 (s, 3H, Ar-CH_3); 1.88−1.84 (m, 2H, Cy-*H*); 1.81 (d, *J* = 6.1 Hz, 3H, O-C*H*-(CH_3)$_2$); 1.78 (d, *J* = 6.1 Hz, 3H, O-C*H*-(CH_3)$_2$); 1.76−1.73 (m, 1H, Cy-*H*); 1.67−1.59 (m, 3H, Cy-*H*); 1.12−1.06 (m, 1H, Cy-*H*); 0.97−0.87 (m, 1H, Cy-*H*). $^{13}C\{^1H\}$ NMR (125 MHz, C_6D_6): δ (only major isomer signals are shown below) 290.9 (Ru=CH-*o*OiPrC_6H_4); 214.0; 152.9; 145.0; 139.9; 138.1; 138.0; 137.5; 136.8; 133.1; 130.6; 129.6; 129.5; 129.2; 122.6; 122.5; 113.2; 75.6; 74.9; 64.9; 63.7; 33.7; 33.4; 33.3; 26.8; 26.6; 22.3; 20.8; 20.8; 20.3; 20.2. Anal. Calcd for $C_{40}H_{46}Cl_2N_2ORu$ (742.78): C, 64.68; H, 6.24; N, 3.77. Found: C, 64.62; H, 6.27; N, 3.81. ESI-FT-ICR (**11c**-Cl): *m*/*z* calcd 707.2342, found 707.2339.

*[(4R,5R)-1-Cyclohexyl-3-mesityl-4,5-diphenylimidazolidinylidene]dichloro(2-isopropoxyphenylmethylene)ruthenium (**12c**).* MW = 742.8 g/mol. Yield: 54%. ^1H NMR (600 MHz, C_6D_6): δ 16.44 (s, 1H, Ru=CH-*o*OiPrC_6H_4); 7.14−7.08 (m, 6H, Ar-*H*); 7.05 (t, *J* = 7.3 Hz, *J* = 7.3 Hz, 1H, Ar-*H*); 7.00−6.94 (m, 5H, Ar-*H*); 6.78 (br s, 1H, Ar-*H*); 6.68 (t, *J* = 7.3 Hz, *J* = 7.5 Hz 1H, Ar-*H*); 6.57 (br s, 1H, Ar-*H*); 6.46 (d, *J* = 8.2 Hz, 1H, Ar-*H*); 5.70 (t t, *J* = 3.1 Hz, *J* = 3.0 Hz, 1H, Cy-*H*); 5.48 (d, *J* = 6.4 Hz, 1H, N-C*H*-CH-N); 4.78 (d, *J* = 6.8 Hz, 1H, N-CH-C*H*-N); 4.71−4.67 (m, 1H, O-C*H*-(CH_3)$_2$); 3.10 (d, *J* = 11.1 Hz, 1H, Cy-*H*); 2.85 (d, *J* = 12.4 Hz, 1H, Cy-*H*); 2.54 (s, 3H, Ar-CH_3); 2.07 (s, 3H, Ar-CH_3); 1.96−1.88 (m, 2H, Cy-*H*); 1.79−1.77 (m, 9H, Ar-CH_3 and O-CH-(CH_3)$_2$); 1.63−1.58 (m, 3H Cy-*H*); 1.00−0.86 (m, 3H Cy-*H*). $^{13}C\{^1H\}$ NMR (125 MHz, C_6D_6): δ 290.2 (Ru=CH-*o*OiPrC_6H_4); 211.8; 153.3; 145.2; 143.3; 141.0; 139.2; 138.8; 137.5; 130.4; 130.2; 129.7; 129.4; 129.3; 129.3; 129.1; 128.9; 122.8; 122.7; 113.5; 79.3; 75.2; 69.6; 64.2; 34.5; 34.3; 32.3; 32.2; 27.4; 26.9; 26.2; 26.1; 22.7; 22.6; 21.3; 21.2; 21.2; 21.1; 20.0; 19.9; 19.5. Anal. Calcd for $C_{40}H_{46}Cl_2N_2ORu$ (742.78): C, 64.68; H, 6.24; N, 3.77. Found C, 64.57; H, 6.34; N, 3.68. ESI-FT-ICR (**12c**-Cl): *m*/*z* calcd 707.2342, found 707.2362.

DOI: 10.1021/acs.organomet.7b00488
Organometallics XXXX, XXX, XXX−XXX

General Procedures for RCM Reactions. An NMR tube with a screw-cap septum top was charged with 0.80 mL of a solution of the catalyst (1−5%) in C_6D_6. After equilibration of the sample at 60 °C in the NMR probe, 0.080 mmol of substrate (0.1 M) was injected into the tube. Conversions of each substrate were monitored over time by ^{1}H NMR.

*RCM of Diethyl Diallylmalonate (**23**) (Figure 5A).* A 19.3 μL portion of **23** was injected into a heated NMR tube containing 0.80 mL of catalyst solution (1 mol %). The conversion to **24** was determined by integrating the methylene protons of the reagent at δ 2.84 (dt) and of the product at δ 3.14 (s).

*RCM of N-Tosyldiallylamine (**25**) (Figure 5B).* A 17.2 μL portion of **25** was injected into a heated NMR tube containing 0.80 mL of catalyst solution (1 mol %). The conversion to **26** was determined by integrating the methylene protons of the reagent at δ 3.71 (d) and of the product at δ 3.90 (s).

*RCM of Diethyl Allylmethallylmalonate (**27**) (Figure 6A).* A 20.5 μL portion of **27** was injected into a heated NMR tube containing 0.80 mL of catalyst solution (1 mol %). The conversion to **28** was determined by integrating the methylene protons of the reagent at δ 2.96(d), 2.93 (s) and of the product at δ 3.18 (m), 3.07 (s).

*RCM of N-Tosylallylmethallylamine (**29**) (Figure 6B).* A 19.4 μL portion of **29** was injected into a heated NMR tube containing 0.80 mL of catalyst solution (1 mol %). The conversion to **30** was determined by integrating the methylene protons of the reagent at δ 3.70(d), 3.67 (s) and of the product at δ 3.96 (m), 3.82 (s).

*RCM of Diethyl Dimethallylmalonate (**31**) (Figure 7A).* A 21.6 μL portion of **31** was injected into a heated NMR tube containing 0.80 mL of catalyst solution (5 mol %). The conversion to **32** was determined by integrating the methylene protons of the reagent at δ 2.98 (s) and of the product at δ 3.15 (s).

*RCM of N-Tosyldimethallylamine (**33**)(Figure 7B).* A 20.2 μL portion of **33** was injected into a heated NMR tube containing 0.80 mL of catalyst solution (5 mol %). The conversion to **34** was determined by integrating the methylene protons of the reagent at δ 3.69 (s) and of the product at δ 3.90 (s).

CM of Allylbenzene (35) and *cis*-1,4-Diacetoxy-2-butene (36) (Scheme 3, Table 3). Under a nitrogen atmosphere, 66 μL of **35** and 160 μL of **36** were added simultaneously to a solution of the catalyst (2.5 mol %) in dry methylene chloride. The reaction mixture was refluxed under nitrogen overnight and then purified by column chromatography with hexane/ethyl acetate 9/1 as eluent. Products **37** and **38** were obtained as transparent oils, and *E*/*Z* ratios were determined by ^{1}H NMR.

Ethenolysis of 39 (Scheme 4, Table 4). Under a nitrogen atmosphere, in an autoclave, **39** (5.4 mmol) and dodecane (150 μL) were introduced. At this point, a t = 0 sample was prepared. The autoclave was purged with ethylene three times, and then a toluene solution of the catalyst (20 to 500 ppm) was added. The autoclave was purged with ethylene three times and then charged with a pressure of 150 psi. The reaction mixture was stirred at 50 or 40 °C for 3 or 2 h and then cooled in an ice bath and quenched with ethyl vinyl ether. After that, GC samples were prepared in hexane. Samples were stored at −20 °C until GC analysis.

ARCM of 44 and 45 without Additive (Scheme 5, Table 5). Under a nitrogen atmosphere, the prochiral triene (0.11 mmol) was added to 2 mL of a CD_2Cl_2 solution of the catalyst (2.5 mol %). A portion of the reaction mixture was transferred in a NMR tube with a J. Young valve and heated at 40 °C for 2 h for **44** and for 3 h for **45**. Yields were determined via NMR spectroscopy of the crude product. The reaction mixture was filtered on neutral alumina and injected into the GC system without further purifications.

ARCM of 44 and 45 with NaI (Scheme 5, Table 5). Under a nitrogen atmosphere, NaI (0.055 mmol) was added to 1 mL of a THF-d_8 solution of the catalyst (4.0 mol %). The reaction mixture was stirred at room temperature for 1 h. Then, the prochiral triene (0.055 mmol) was added and then the mixture was transferred to an NMR tube with a J. Young valve and heated at 40 °C for 2 h for **44** and for 3 h for **45**. Yields were determined via NMR spectroscopy of the crude product. The reaction mixture was filtered on neutral alumina and injected into the GC system without further purifications.

AROCM of 48 with Styrene (Scheme 6, Table 6). Under a nitrogen atmosphere, **48** (0.43 mol) and styrene (4.3 mmol) were simultaneously added to 7.5 mL of a CH_2Cl_2 solution of the catalyst (3 mol %). The reaction mixture was stirred at room temperature for 3 h and then concentrated and purified via column chromatography (petroleum ether/diethyl ether 1/1) to afford the product as a transparent oil. About 1.3 mg of the product was dissolved in 2 mL of hexane/2-propanol 1/1 (HPLC grade purity), filtered using a syringe filter, and then injected into the HPLC system.

■ ASSOCIATED CONTENT

Supporting Information

The Supporting Information is available free of charge on the ACS Publications website at DOI: 10.1021/acs.organomet.7b00488.

Experimental procedures, figures giving NMR spectra of the new complexes, GC and HPLC chromatograms of ethenolysis reaction mixture, **46**, **47**, and **49**, and experimental details for complexes **47** and **48** (PDF)

Cartesian coordinates for the optimized structures (XYZ)

Accession Codes

CCDC 1533652−1533654 contain the supplementary crystallographic data for this paper. These data can be obtained free of charge via www.ccdc.cam.ac.uk/data_request/cif, or by emailing data_request@ccdc.cam.ac.uk, or by contacting The Cambridge Crystallographic Data Centre, 12 Union Road, Cambridge CB2 1EZ, UK; fax: +44 1223 336033.

■ AUTHOR INFORMATION

Corresponding Author

*E-mail for F.G.: fgrisi@unisa.it.

ORCID

Chiara Costabile: 0000-0001-8538-7125

Fabia Grisi: 0000-0003-3904-9541

Notes

The authors declare no competing financial interest.

■ ACKNOWLEDGMENTS

The authors thank Dr. Patrizia Iannece, Dr. Ivano Immediata, and Patrizia Oliva for technical assistance. This work was financed by the Ministero dell'Università e della Ricerca Scientifica e Tecnologica. Financial support from POR CAMPANIA FESR 2007/2013 O.O.2.1.-CUP B46D14002660009 "Il potenziamento e la riqualificazione del sistema delle infrastrutture nel settore dell'istruzione, della formazione e della ricerca" is gratefully acknowledged. M.D. and K.G. acknowledge the National Science Centre (Poland) for the NCN MAESTRO Grant No. DEC-2012/04A/ST5/00594.

■ REFERENCES

(1) (a) Grela, K. *Olefin Metathesis: Theory and Practice*; Wiley: Hoboken, NJ, 2014. (b) Grubbs, R. H.; Wenzel, A. G.; O'Leary, D. J.; Khosravi, E. *Handbook of Metathesis*, 2nd ed.; Wiley-VCH: Weinheim, Germany, 2015.

(2) (a) Scholl, M.; Ding, S.; Lee, C. W.; Grubbs, R. H. Synthesis and Activity of a New Generation of Ruthenium-Based Olefin Metathesis Catalysts Coordinated with 1,3-Dimesityl-4,5-dihydroimidazol-2-ylidene Ligands. *Org. Lett.* **1999**, *1* (6), 953−956. (b) Garber, S. B.; Kingsbury, J. S.; Gray, B. L.; Hoveyda, A. H. Efficient and Recyclable

DOI: 10.1021/acs.organomet.7b00488
Organometallics XXXX, XXX, XXX−XXX

Monomeric and Dendritic Ru-Based Metathesis Catalysts. *J. Am. Chem. Soc.* **2000**, *122* (34), 8168−8179. (c) Jafarpour, L.; Schanz, H. J.; Stevens, E. D.; Nolan, S. P. Indenylidene−Imidazolylidene Complexes of Ruthenium as Ring-Closing Metathesis Catalysts. *Organometallics* **1999**, *18* (25), 5416−5419.

(3) (a) Cossy, J.; Arseniyadis, S.; Meyer, C. *Metathesis in Natural Product Synthesis*; Wiley-VCH: Weinheim, Germany, 2010. (b) Nickel, A.; Ung, T.; Mkrtumyan, G.; Uy, J.; Lee, C.; Stoianova, D.; Papazian, J.; Wei, W.-H.; Mallari, A.; Schrodi, Y.; Pederson, R. L A. Highly Efficient Olefin Metathesis Process for the Synthesis of Terminal Alkenes from Fatty Acid Esters. *Top. Catal.* **2012**, *55* (7), 518−523. (c) Chikkali, S.; Mecking, S. Refining of Plant Oils to Chemicals by Olefin Metathesis. *Angew. Chem., Int. Ed.* **2012**, *51* (24), 5802−5808. (d) de Espinosa, L. M.; Meier, M. A. R. Olefin Metathesis of Renewable Platform Chemicals. *Top. Organomet. Chem.* **2012**, *39*, 1−44. (e) Higman, C. S.; Lummiss, J. A. M.; Fogg, D. E. Olefin Metathesis at the Dawn of Implementation in Pharmaceutical and Specialty-Chemicals Manufacturing. *Angew. Chem., Int. Ed.* **2016**, *55* (11), 3552−3565. (f) Bidange, J.; Fischmeister, C.; Bruneau, C. Ethenolysis: A Green Catalytic Tool to Cleave Carbon-Carbon Double Bonds. *Chem. - Eur. J.* **2016**, *22* (35), 12226−12244. (g) Rouen, M.; Queval, P.; Borré, E.; Falivene, L.; Poater, A.; Berthod, M.; Hugues, F.; Cavallo, L.; Baslé, O.; Olivier-Bourbigou, H.; Mauduit, M. Selective Metathesis of α-Olefins from Bio-Sourced Fischer−Tropsch Feeds. *ACS Catal.* **2016**, *6* (11), 7970−7976.

(4) (a) Vougioukalakis, G. C.; Grubbs, R. H. Ruthenium-Based Heterocyclic Carbene-Coordinated Olefin Metathesis Catalysts. *Chem. Rev.* **2010**, *110* (3), 1746−1787. (b) Samojlowicz, C.; Bieniek, M.; Grela, K. Ruthenium-Based Olefin Metathesis Catalysts Bearing N-Heterocyclic Carbene Ligands. *Chem. Rev.* **2009**, *109* (8), 3708−3742. (c) Paradiso, V.; Costabile, C.; Grisi, F. NHC backbone configuration in ruthenium-catalyzed olefin metathesis. *Molecules* **2016**, *21* (1), 117−136.

(5) (a) Chung, C. K.; Grubbs, R. H. Olefin Metathesis Catalyst: Stabilization Effect of Backbone Substitutions of N-Heterocyclic Carbene. *Org. Lett.* **2008**, *10* (13), 2693−2696. (b) Kuhn, K. M.; Bourg, J.-B.; Chung, C. K.; Virgil, S. C.; Grubbs, R. H. Effects of NHC-Backbone Substitution on Efficiency in Ruthenium-Based Olefin Metathesis. *J. Am. Chem. Soc.* **2009**, *131* (14), 5313−5320. (c) Grisi, F.; Mariconda, A.; Costabile, C.; Bertolasi, V.; Longo, P. Influence of *syn* and *anti* Configurations of NHC Backbone on Ru-Catalyzed Olefin Metathesis. *Organometallics* **2009**, *28* (17), 4988−4995. (d) Costabile, C.; Mariconda, A.; Cavallo, L.; Longo, P.; Bertolasi, V.; Ragone, F.; Grisi, F. The Pivotal Role of Symmetry in the Ruthenium-Catalyzed Ring-Closing Metathesis of Olefins. *Chem. - Eur. J.* **2011**, *17* (31), 8618−8629. (e) Perfetto, A.; Costabile, C.; Longo, P.; Bertolasi, V.; Grisi, F. Probing the Relevance of NHC Ligand Conformations in the Ru-Catalysed Ring-Closing Metathesis Reaction. *Chem. - Eur. J.* **2013**, *19* (32), 10492−10496. (f) Borguet, Y.; Zaragoza, G.; Demonceau, A.; Delaude, L. Ruthenium catalysts bearing a benzimidazolylidene ligand for the metathetical ring-closure of tetrasubstituted cycloolefins. *Dalton Trans.* **2015**, *44* (21), 9744−9755.

(6) (a) Tornatzky, J.; Kannenberg, A.; Blechert, S. New catalysts with unsymmetrical N-heterocyclic carbene ligands. *Dalton Trans.* **2012**, *41* (27), 8215−8225. (b) Hamad, F. B.; Sun, T.; Xiao, S.; Verpoort, F. Olefin metathesis ruthenium catalysts bearing unsymmetrical heterocylic carbenes. *Coord. Chem. Rev.* **2013**, *257* (15−16), 2274−2292. (c) Shahane, S.; Bruneau, C.; Fischmeister, C. Z Selectivity: Recent Advances in one of the Current Major Challenges of Olefin Metathesis. *ChemCatChem* **2013**, *5* (12), 3436−3459. (d) Montgomery, T. P.; Johns, A. M.; Grubbs, R. H. Recent Advancements in Stereoselective Olefin Metathesis Using Ruthenium Catalysts. *Catalysts* **2017**, *7* (3), 87−124.

(7) Selected examples of *N*-alkyl/*N*-aryl NHC-Ru complexes: (a) Dinger, M. B.; Nieczypor, P.; Mol, J. C. Adamantyl-Substituted N-Heterocyclic Carbene Ligands in Second-Generation Grubbs-Type Metathesis Catalysts. *Organometallics* **2003**, *22* (25), 5291−5296. (b) Vehlow, K.; Maechling, S.; Blechert, S. Ruthenium Metathesis Catalysts with Saturated Unsymmetrical N-Heterocyclic Carbene Ligands. *Organometallics* **2006**, *25* (1), 25−28. (c) Ledoux, N.; Allaert, B.; Pattyn, S.; Mierde, H. V.; Vercaemst, C.; Verpoort, F. N,N′-Dialkyl- and N-Alkyl-N-mesityl-Substituted N-Heterocyclic Carbenes as Ligands in Grubbs Catalysts. *Chem. - Eur. J.* **2006**, *12* (17), 4654−4661. (d) Thomas, R. M.; Keitz, B. K.; Champagne, T. M.; Grubbs, R. H. Highly Selective Ruthenium Metathesis Catalysts for Ethenolysis. *J. Am. Chem. Soc.* **2011**, *133* (19), 7490−7496. (e) Ablialimov, O.; Kędziorek, M.; Torborg, C.; Malińska, M.; Woźniak, K.; Grela, K. New Ruthenium(II) Indenylidene Complexes Bearing Unsymmetrical N-Heterocyclic Carbenes. *Organometallics* **2012**, *31* (21), 7316−7319. (f) Rouen, M.; Borre, E.; Falivene, L.; Toupet, L.; Berthod, M.; Cavallo, L.; Olivier-Bourbigou, H.; Mauduit, M. Cycloalkyl-based unsymmetrical unsaturated (U2)-NHC ligands: flexibility and dissymmetry in ruthenium-catalysed olefin metathesis. *Dalton Trans.* **2014**, *43* (19), 7044−7049. (g) Yu, B.; Hamad, F. B.; Sels, B.; Van Hecke, K.; Verpoort, F. Ruthenium indenylidene complexes bearing N-alkyl/N-mesityl-substituted N-heterocyclic carbene ligands. *Dalton Trans.* **2015**, *44* (26), 11835−11842.

(8) (a) Van Veldhuizen, J. J.; Gillingham, D. G.; Garber, S. B.; Kataoka, O.; Hoveyda, A. H. Chiral Ru-Based Complexes for Asymmetric Olefin Metathesis: Enhancement of Catalyst Activity through Steric and Electronic Modifications. *J. Am. Chem. Soc.* **2003**, *125* (41), 12502−12508. (b) Fournier, P.-A.; Collins, S. K. A Highly Active Chiral Ruthenium-Based Catalyst for Enantioselective Olefin Metathesis. *Organometallics* **2007**, *26* (12), 2945−2949. (c) Tiede, S.; Berger, A.; Schlesiger, D.; Rost, D.; Lühl, A.; Blechert, S. Highly Active Chiral Ruthenium-Based Metathesis Catalysts through a Monosubstitution in the N-Heterocyclic Carbene. *Angew. Chem., Int. Ed.* **2010**, *49* (23), 3972−3975. (d) Hartung, J.; Dornan, P. K.; Grubbs, R. H. Enantioselective Olefin Metathesis with Cyclometalated Ruthenium Complexes. *J. Am. Chem. Soc.* **2014**, *136* (37), 13029−13037.

(9) (a) Vehlow, K.; Wang, D.; Buchmeiser, M. R.; Blechert, S. Alternating Copolymerizations Using a Grubbs-Type Initiator with an Unsymmetrical, Chiral N-Heterocyclic Carbene Ligand. *Angew. Chem., Int. Ed.* **2008**, *47* (14), 2615−2618. (b) Engl, P. S.; Fedorov, A.; Coperet, C.; Togni, A. N-Trifluoromethyl NHC Ligands Provide Selective Ruthenium Metathesis Catalysts. *Organometallics* **2016**, *35* (6), 887−893.

(10) Kavitake, S.; Samantaray, M. K.; Dehn, R.; Deuerlein, S.; Limbach, M.; Schachner, J. A.; Jeanneau, E.; Copéret, C.; Thieuleux, C. Unsymmetrical Ru-NHC catalysts: a key for the selective tandem Ring Opening−Ring Closing alkene Metathesis (RO−RCM) of cyclooctene. *Dalton Trans.* **2011**, *40* (46), 12443−12446.

(11) Herbert, M. B.; Grubbs, R. H. Z-Selective Cross Metathesis with Ruthenium Catalysts: Synthetic Applications and Mechanistic Implications. *Angew. Chem., Int. Ed.* **2015**, *54* (17), 5018−5024.

(12) (a) Ablialimov, O.; Kędziorek, M.; Malińska, M.; Woźniak, K.; Grela, K. Synthesis, Structure, and Catalytic Activity of New Ruthenium(II) Indenylidene Complexes Bearing Unsymmetrical N-Heterocyclic Carbenes. *Organometallics* **2014**, *33* (9), 2160−2171. (b) Smoleń, M.; Kośnik, W.; Loska, R.; Gajda, R.; Malińska, M.; Woźniak, K.; Grela, K. Synthesis and catalytic activity of ruthenium indenylidene complexes bearing unsymmetrical NHC containing a heteroaromatic moiety. *RSC Adv.* **2016**, *6* (80), 77013−77019.

(13) (a) Paradiso, V.; Bertolasi, V.; Grisi, F. Novel Olefin Metathesis Ruthenium Catalysts Bearing Backbone Substituted Unsymmetrical NHC Ligands. *Organometallics* **2014**, *33* (21), 5932−5935. (b) Paradiso, V.; Bertolasi, V.; Costabile, C.; Grisi, F. Ruthenium olefin metathesis catalysts featuring unsymmetrical N-heterocyclic carbenes. *Dalton Trans.* **2016**, *45* (2), 561−571.

(14) Parsons, S.; Flack, H.; Wagner, T. Use of intensity quotients and differences in absolute structure refinement. *Acta Crystallogr., Sect. B: Struct. Sci., Cryst. Eng. Mater.* **2013**, *69*, 249−259.

(15) Burnett, M. N.; Johnson, C. K. *ORTEP III*; Oak Ridge National Laboratory, Oak Ridge, TN, 1996; Report ORNL-6895.

(16) Dichloro[1,3-bis(2,4,6-trimethylphenyl)-2-imidazolidinylidene](2-isopropoxyphenyl methylene)ruthenium(II) (**HGII**).

(17) Under the employed conditions, after 1 month 100% of **11c** and **12c** still persisted, while 79% of **HGII** was undecomposed.

DOI: 10.1021/acs.organomet.7b00488
Organometallics XXXX, XXX, XXX−XXX

(18) Małecki, P.; Gajda, K.; Ablialimov, O.; Malińska, M.; Gajda, R.; Woźniak, K.; Kajetanowicz, A.; Grela, K. Hoveyda-Grubbs Type Precatalysts with Unsymmetrical N-Heterocyclic Carbenes as Effective Catalysts in Olefin Metathesis. *Organometallics* **2017**, *36* (11), 2153−2166.
(19) Wu. M, M.; Gill, A. M.; Yunpeng, L.; Falivene, L.; Yongxin, L.; Ganguly, R.; Cavallo, L.; Garcìa, F. Synthesis, structural studies and ligand influence on the stability of aryl-NHC stabilized trimethylaluminium complexes. *Dalton Trans.* **2015**, *44* (34), 15166−15174.
(20) Falivene, L.; Credendino, R.; Poater, A.; Petta, A.; Serra, L.; Oliva, R.; Scarano, V.; Cavallo, L. SambVca 2. A Web Tool for Analyzing Catalytic Pockets with Topographic Steric Maps. *Organometallics* **2016**, *35* (13), 2286−2293.
(21) (a) Dorta, R.; Stevens, E. D.; Scott, N. M.; Costabile, C.; Cavallo, L.; Hoff, C. D.; Nolan, S. P. Steric and Electronic Properties of N-Heterocyclic Carbenes (NHC): A Detailed Study on Their Interaction with $Ni(CO)_4$. *J. Am. Chem. Soc.* **2005**, *127* (8), 2485−2495. (b) Cavallo, L.; Correa, A.; Costabile, C.; Jacobsen, H. Steric and electronic effects in the bonding of N-heterocyclic ligands to transition metals. *J. Organomet. Chem.* **2005**, *690* (24−25), 5407−5413. (c) Jacobsen, H.; Correa, A.; Poater, A.; Costabile, C.; Cavallo, L. Understanding the M (NHC) (NHC = N-heterocyclic carbene) bond. *Coord. Chem. Rev.* **2009**, *253* (21−22), 687−703.
(22) (a) Hong, S. H.; Chlenov, A.; Day, M. W.; Grubbs, R. H. Double C-H activation of an N-heterocyclic carbene ligand in a ruthenium olefin metathesis catalyst. *Angew. Chem., Int. Ed.* **2007**, *46* (27), 5148−5151. (b) Mathew, J.; Koga, N.; Suresh, C. H. C-H Bond Activation through σ-Bond Metathesis and Agostic Interactions: Deactivation Pathway of a Grubbs Second-Generation Catalyst. *Organometallics* **2008**, *27* (18), 4666−4670.
(23) Cannon, J. S.; Zou, L.; Liu, P.; Lan, Y.; O'Leary, D. J.; Houk, K. N.; Grubbs, R. H. Carboxylate-Assisted C(sp3)−H Activation in Olefin Metathesis-Relevant Ruthenium Complexes. *J. Am. Chem. Soc.* **2014**, *136* (18), 6733−6743.
(24) Süßner, M.; Plenio, H. π-Face donor properties of N-heterocyclic carbenes. *Chem. Commun.* **2005**, *43*, 5417−5419.
(25) Perfetto, A.; Bertolasi, V.; Costabile, C.; Paradiso, V.; Caruso, T.; Longo, P.; Grisi, F. Methyl and Phenyl Substituent Effects on the Catalytic Behavior of NHC Ruthenium Complexes. *RSC Adv.* **2016**, *6* (98), 95793−95804.
(26) Fournier, P.-A.; Savoie, J.; Stenne, B.; Bédard, M.; Grandbois, A.; Collins, S. K. Mechanistically Inspired Catalysts for Enantioselective Desymmetrizations by Olefin Metathesis. *Chem. - Eur. J.* **2008**, *14* (28), 8690−8695.
(27) (a) Mol, J. C. Application of olefin metathesis in oleochemistry: an example of green chemistry. *Green Chem.* **2002**, *4* (1), 5−13. (b) Spekreijse, J.; Sanders, J. P. M.; Bitter, J. H.; Scott, E. L. The Future of Ethenolysis in Biobased Chemistry. *ChemSusChem* **2017**, *10* (3), 470−482.
(28) (a) Stewart, I. C.; Keitz, B. K.; Kuhn, K. M.; Thomas, R. M.; Grubbs, R. H. Nonproductive Events in Ring-Closing Metathesis Using Ruthenium Catalysts. *J. Am. Chem. Soc.* **2010**, *132* (25), 8534−8535. (b) Keitz, B. K.; Grubbs, R. H. Probing the Origin of Degenerate Metathesis Selectivity via Characterization and Dynamics of Ruthenacyclobutanes Containing Variable NHCs. *J. Am. Chem. Soc.* **2011**, *133* (40), 16277−16284.
(29) (a) Anderson, D. R.; Lavallo, V.; O'Leary, D. J.; Bertrand, G.; Grubbs, R. H. Synthesis and reactivity of olefin metathesis catalysts bearing cyclic (alkyl)(amino)carbenes. *Angew. Chem., Int. Ed.* **2007**, *46* (38), 7262−7265. (b) Anderson, D. R.; Ung, T.; Mkrtumyan, G.; Bertrand, G.; Grubbs, R. H. Kinetic Selectivity of Olefin Metathesis Catalysts Bearing Cyclic (Alkyl)(Amino)Carbenes. *Organometallics* **2008**, *27*, 563−566. (c) Schrodi, Y.; Ung, T.; Vargas, A.; Mkrtumyan, G.; Lee, W.-C.; Champagne, T. M.; Pederson, R. L.; Hong, S. H. Ruthenium Olefin Metathesis Catalysts for the Ethenolysis of Renewable Feedstocks. *Clean: Soil, Air, Water* **2008**, *36* (8), 669−673. (d) Zhang, J.; Song, S.; Wang, X.; Jiao, J.; Shi, M. Ruthenium-catalyzed olefin metathesis accelerated by the steric effect of the backbone substituent in cyclic (alkyl)(amino) carbenes. *Chem. Commun.* **2013**, *49*, 9491−9493. (e) Marx, V. M.; Sullivan, A. H.; Melaimi, M.; Virgil, S. C.; Keitz, B. K.; Weinberger, D. S.; Bertrand, G.; Grubbs, R. H. Cyclic alkyl amino carbene (CAAC) ruthenium complexes as remarkably active catalysts for ethenolysis. *Angew. Chem., Int. Ed.* **2015**, *54* (6), 1919−1923. (f) Gawin, R.; Kozakiewicz, A.; Guńka, P. A.; Dąbrowski, P.; Skowerski, K. Bis(Cyclic Alkyl Amino Carbene) Ruthenium Complexes: A Versatile, Highly Efficient Tool for Olefin Metathesis. *Angew. Chem., Int. Ed.* **2017**, *56* (4), 981−986.
(30) Only enantiopure *anti* catalysts were tested due to the difficulty in separating racemic mixtures of *syn* isomers, although preliminary studies to evaluate the effect of *syn* and *anti* stereochemical relationships of substituents on the backbone of uNHC have been undertaken by some of us. See: Paradiso, V.; Menta, S.; Pierini, M.; Della Sala, G.; Ciogli, A.; Grisi, F. Enantiopure C1-symmetric N-Heterocyclic Carbene Ligands from desymmetrized meso-1,2-Diphenylethylenediamine: Application in Ruthenium- Catalyzed Olefin Metathesis. *Catalysts* **2016**, *6* (11), 177.
(31) (a) Seiders, T. J.; Ward, D. W.; Grubbs, R. H. Enantioselective Ruthenium-Catalyzed Ring-Closing Metathesis. *Org. Lett.* **2001**, *3* (20), 3225−3228. (b) Funk, T. W.; Berlin, J. M.; Grubbs, R. H. Highly Active Chiral Ruthenium Catalysts for Asymmetric Ring-Closing Olefin Metathesis. *J. Am. Chem. Soc.* **2006**, *128* (6), 1840−1846.
(32) Stenne, B.; Timperio, J.; Savoie, J.; Dudding, T.; Collins, S. K. Desymmetrizations Forming Tetrasubstituted Olefins Using Enantioselective Olefin Metathesis. *Org. Lett.* **2010**, *12* (9), 2032−2035.
(33) (a) Van Veldhuizen, J. J.; Garber, S. B.; Kingsbury, J. S.; Hoveyda, A. H. A Recyclable Chiral Ru Catalyst for Enantioselective Olefin Metathesis. Efficient Catalytic Asymmetric Ring-Opening/Cross Metathesis in Air. *J. Am. Chem. Soc.* **2002**, *124* (18), 4954−4955. (b) Berlin, J. M.; Goldberg, S. D.; Grubbs, R. H. Highly Active Chiral Ruthenium Catalysts for Asymmetric Cross- and Ring-Opening Cross-Metathesis. *Angew. Chem., Int. Ed.* **2006**, *45* (45), 7591−7595. (c) Tiede, S.; Berger, A.; Schlesiger, D.; Rost, D.; Lühl, A.; Blechert, S. Highly Active Chiral Ruthenium-Based Metathesis Catalysts through a Monosubstitution in the N-Heterocyclic Carbene. *Angew. Chem., Int. Ed.* **2010**, *49* (23), 3972−3975.
(34) Thomas, R. M.; Grubbs, R. H. Mechanistic Studies of Enantioselective N-aryl, N-alkyl NHC Ruthenium Metathesis Catalysts in Asymmetric Ring-Opening Cross-Metathesis. *Chem. New Zealand* **2011**, *75* (2), 65−71.
(35) Gatti, M.; Vieille-Petit, L.; Xinjun, L.; Mariz, R.; Drinkel, E.; Linden, A.; Dorta, R. Impact of NHC Ligand Conformation and Solvent Concentration on the Ruthenium-Catalyzed Ring-Closing Metathesis Reaction. *J. Am. Chem. Soc.* **2009**, *131* (27), 9498−9499.
(36) Rodrigues, C. A. B.; Norton de Matos, M.; Guerreiro, B. M. H.; Gonçalves, A. M. L.; Romão, C. C.; Afonso, C. A. M. Water as efficient medium for mild decarbonylation of tertiary aldehydes. *Tetrahedron Lett.* **2011**, *52* (22), 2803−2807.
(37) Frisch, M. J.; Trucks, G. W.; Schlegel, H. B.; Scuseria, G. E.; Robb, M. A.; Cheeseman, J. R.; Scalmani, G.; Barone, V.; Mennucci, B.; Petersson, G. A.; Nakatsuji, H.; Caricato, M.; Li, X.; Hratchian, H. P.; Izmaylov, A. F.; Bloino, J.; Zheng, G.; Sonnenberg, J. L.; Hada, M.; Ehara, M.; Toyota, K.; Fukuda, R.; Hasegawa, J.; Ishida, M.; Nakajima, T.; Honda, Y.; Kitao, O.; Nakai, H.; Vreven, T.; Montgomery, J. A., Jr.; Peralta, J. E.; Ogliaro, F.; Bearpark, M.; Heyd, J. J.; Brothers, E.; N. Kudin, K.; Staroverov, V. N.; Kobayashi, R.; Normand, J.; Raghavachari, K.; Rendell, A.; Burant, J. C.; Iyengar, S. S.; Tomasi, J.; Cossi, M.; Rega, N.; Millam, J. M.; Klene, M.; Knox, J. E.; Cross, J. B.; Bakken, V.; Adamo, C.; Jaramillo, J.; Gomperts, R.; Stratmann, R. E.; Yazyev, O.; Austin, A. J.; Cammi, R.; Pomelli, C.; Ochterski, J. W.; Martin, R. L.; Morokuma, K.; Zakrzewski, V. G.; Voth, G. A.; Salvador, P.; Dannenberg, J. J.; Dapprich, S.; Daniels, A. D.; Farkas, O.; Foresman, J. B.; Ortiz, J. V.; Cioslowski, J.; Fox, D. J. *Gaussian 09, Revision A.02*; Gaussian, Inc., Wallingford, CT, 2009.
(38) (a) Becke, A. D. Density-functional exchange-energy approximation with correct asymptotic behavior. *Phys. Rev. A: At., Mol., Opt. Phys.* **1988**, *38* (6), 3098−3100. (b) Perdew, J. P. Density-functional approximation for the correlation energy of the inhomogeneous electron gas. *Phys. Rev. B: Condens. Matter Mater. Phys.* **1986**, *33* (12),

DOI: 10.1021/acs.organomet.7b00488
Organometallics XXXX, XXX, XXX−XXX

8822−8824. (c) Perdew, J. P. Density-functional approximation for the correlation energy of the inhomogeneous electron gas. *Phys. Rev. B: Condens. Matter Mater. Phys.* **1986**, *34* (13), 7406−7406. (d) Capobianco, A.; Caruso, T.; Peluso, A. Hole delocalization over adenine tracts in single stranded DNA oligonucleotides. *Phys. Chem. Chem. Phys.* **2015**, *17*, 4750−4756.

(39) Schaefer, A.; Horn, H.; Ahlrichs, R. J. Fully optimized contracted Gaussian basis sets for atoms Li to Kr. *J. Chem. Phys.* **1992**, *97* (4), 2571−2577.

(40) (a) Haussermann, U.; Dolg, M.; Stoll, H.; Preuss, H. Accuracy of energy-adjusted quasirelativistic ab initio pseudopotentials: all-electron and pseudopotential benchmark calculations for Hg, HgH and their cations. *Mol. Phys.* **1993**, *78* (5), 1211−1224. (b) Kuechle, W.; Dolg, M.; Stoll, H.; Preuss, H. J. Energy-adjusted pseudopotentials for the actinides. Parameter sets and test calculations for thorium and thorium monoxide. *J. Chem. Phys.* **1994**, *100* (10), 7535−7542. (c) Leininger, T.; Nicklass, A.; Stoll, H.; Dolg, M.; Schwerdtfeger, P. The accuracy of the pseudopotential approximation. II. A comparison of various core sizes for indium pseudopotentials in calculations for spectroscopic constants of InH, InF, and InCl. *J. Chem. Phys.* **1996**, *105* (3), 1052−1059.

DOI: 10.1021/acs.organomet.7b00488
Organometallics XXXX, XXX, XXX−XXX